False Discovery Rate-Adjusted Charting Schemes for Multistage Process Monitoring and Fault Identification

Yanting LI

Department of Industrial Engineering
and Management
Shanghai Jiao Tong University
Shanghai, China
(*ytli@sjtu.edu.cn*)

Fugee TSUNG

Department of Industrial Engineering
and Logistics Management
Hong Kong University of Science and Technology
Kowloon, Hong Kong
(*season@ust.hk*)

Most statistical process control research focuses on single-stage processes. This article considers the problem of multistage process monitoring and fault identification. This problem is formulated as a multiple hypotheses testing problem; however, as the number of stages increases, the detection power of multiple hypotheses testing methods that seek to control the type I error rate decreases dramatically. To maintain the detection power, we use a *false discovery rate* (FDR) control approach, which is widely used in microarray research. Two multistage process monitoring and fault identification schemes—an FDR-adjusted Shewhart chart and an FDR-adjusted cumulative sum (CUSUM) chart—are established. To apply the FDR approach, the distribution of the CUSUM statistics are obtained based on Markov chain theory and Brownian motion with drift models. The detection and fault identification power of the new schemes are evaluated by the Monte Carlo method. The results indicate that the novel FDR-adjusted approaches are better at identifying the faulty stage than the conventional type I error rate control approach, especially when multiple out-of-control stages are present.

KEY WORDS: Distribution of the CUSUM statistic; False discovery rate; Multistage process; State-space model.

1. INTRODUCTION

As modern technology becomes increasingly sophisticated, most manufacturing processes, including those producing printed circuit boards, semiconductors, automobiles, and aerospace products, include numerous operating stages. For example, the dielectric layer formulation process in the semiconductor manufacturing industry comprises the sequential stages of spin coating, soft baking, exposing, developing, curing, and plasma descumming (Kim and May 1999), and up to hundreds of stages are involved in the automobile assembly process. Because the demand for professional customer service requires detailed division of labor, multistage processes can now be found in service industries as well. For example, in an international shipping terminal, the vessel discharging service is characterized by multiple stages; the quay cranes first unload the containers from vessels to tractors, then the tractors transport the containers to the container yard; and the yard cranes then unload the containers from the tractors onto the stacks. In most cases, multistage processes have a unique cascading property (Hawkins 1993); that is, outputs from operations in the upstream stages may affect the quality of the downstream stages, and a product or service variation may propagate throughout the production or service stages.

Thanks to recent advances in sensing and information technologies, automatic data acquisition techniques are now commonly used in many modern processes with multiple stages, and large amounts of data and information related to quality measurements have become available. Thus statistical process control (SPC) to make use of multistage process data and information has become possible. In this work we sought to establish SPC schemes that efficiently monitor and diagnose multistage processes involving a large number of stages.

SPC methods are widely used in manufacturing and service industries for monitoring and diagnosis purposes. But most SPC research and practices focus on monitoring the output of a single stage or the quality dimensions of finished products; work on multistage process monitoring and diagnosis has been limited. Existing SPC methods for multistage process monitoring include two popular approaches, the regression adjustment method and the cause-selecting method. The regression adjustment method, developed by Hawkins (1991, 1993) and applied by Hauck, Runger, and Montgomery (1999), Rao et al. (1996), and others, is applicable because of its ability to tackle the cascading property of a multistage process. Process quality variables are regressed on any subset of the other quality variables. The residuals from the regression models of each stage can then be charted and monitored. Alternatively, Zhang (1984, 1985, 1989, 1992) proposed the cause-selecting method, which is similar in principle to the regression adjustment approach but with the quality variable at the current stage regressed only on that in the previous stage. This cause-selecting method has been reviewed by Wade and Woodall (1993). Recent research into the use of cause-selecting charts for multistage processes includes that of Shu, Apley, and Tsung (2003), Shu and Tsung (2003), and Shu, Tsung, and Kapur (2004). Similarly, Zantek, Wright, and Plante (2002, 2006) regressed the

TECHNOMETRICS, MAY 2009, VOL. 51, NO. 2
DOI 10.1198/TECH.2009.0019

quality characteristics of each stage on all of the quality characteristics in the preceding stages, and then constructed cumulative sum (CUSUM) charts (Page 1954) on the residuals from the regression model of each stage.

Although existing SPC methods for multistage process monitoring are popular, a drawback of these methods is that the statistical models that they use to describe the multistage processes usually lack an engineering background and and cannot describe the relationship among stages explicitly. In an attempt to resolve this problem, several studies on multistage processes have adopted engineering models with linear state-space model structures because of their capability to incorporate physical laws and engineering knowledge to describe the quality linkage among multiple stages in a process. Jin and Shi (1999) and Ding, Shi, and Ceglarek (2002) used this structure to consider a rigid-part assembly process. Djurdjanovic and Ni (2001), Huang, Zhou, and Shi (2002), and Zhou, Huang, and Shi (2003) used this structure to analyze multistage machining processes. Lawless, Mackay, and Robinson (1999) and Agrawal, Lawless, and Mackay (1999) discussed a car hood assembly process that could be put into a linear state-space structure to represent variation transmission across stages (Xiang and Tsung 2008).

Some multistage process diagnosis methods also adopt the linear state-space model. Ding, Ceglarek, and Shi (2002) proposed a method to map the feature patterns of real production data with predetermined fault patterns generated from the analytical model. Ding, Shi, and Ceglarek (2002) and Zhou et al. (2003) investigated the diagnosability of a multistage process, which is the ability to distinguish predetermined specific faults in a multistage process. In contrast, the focus of the present article is on distinguishing and identifying the faulty stages, rather than specific faults, after an out-of-control signal, a topic that has not been reported in the literature to date. As the number of stages increases, effectively and efficiently identifying the faulty stages responsible for changes in a multistage process can be quite challenging.

A few other multistage process monitoring and diagnosis methods also adopt the linear state-space model. Zou and Tsung (2008) utilized directional information based on multistage state space model and proposed multiple MEWMA scheme for effective process monitoring and fault diagnosis. By combining the same directional information and multivariate two sample test, Zou, Tsung, and Liu (2008) proposed a novel change point approach for Phase I analysis of multistage process. However, their method fails when more than one fault occurs in the process. In this article, we try to design a multistage process monitoring scheme that is applicable even in presence of multiple fault. Ding, Ceglarek, and Shi (2002) proposed a method to map the feature patterns of real production data with predetermined fault patterns generated from the analytical model. Ding, Shi, and Ceglarek (2002) and Zhou et al. (2003) investigated the diagnosability of a multistage process, which is the ability to distinguish predetermined specific faults in a multistage process. In contrast, the focus of the present article is on distinguishing and identifying the faulty stages, rather than specific faults, after an out-of-control signal, a topic that has not been reported in the literature to date. As the number of stages increases, effectively and efficiently identifying the faulty stages responsible for changes in a multistage process can be quite challenging.

To tackle the multiplicity problems caused by a large number of hypotheses, Benjamini and Hochberg (1995) proposed a novel approach to the problem of multiple hypotheses testing using false discovery rate (FDR) control. FDR is used to quantify the expected ratio of erroneous rejections to the number of all of the rejected hypotheses. It has been theoretically proven that when the number of hypotheses is large, controlling FDR is much more powerful than controlling the traditional type I error rate. When all of the null hypotheses are exactly true (which is not realistic for the settings that we consider), controlling the FDR is equivalent to controlling the type I error rate. When some of the alternative hypotheses are true, as in practical applications, controlling the FDR can provide much higher power. Recent research on FDR control has been reported by Benjamini and Liu (1999), Benjamini and Hochberg (2000), Benjamini and Yekutieli (2001, 2005), Genovese and Wasserman (2002), Benjamini, Krieger, and Yekutieli (2006), Storey (2001, 2002), and Storey, Taylor, and Siegmund (2004). FDR has been extensively studied and applied in many fields, including microarray research, which usually involves simultaneously comparing up to thousands of individual DNA sequences (e.g., Tusher, Tibshirani, and Chu 2001; Reiner, Yekutieli, and Benjamini 2003; Qian and Huang 2005; Grant, Liu, and Stoeckert 2005).

Earlier work applying FDR control to SPC can be traced back to Benjamini and Kling (1999), who investigated the advantages of using p-values in statistical control charts. Marshall et al. (2004) applied multiple CUSUM charts in health care surveillance, such as monitoring hospital units and doctors. Grigg and Spiegelhalter (2005) established random-effects CUSUM charts for hospital mortality monitoring using FDR as a performance evaluation criterion. As pointed out by Woodall (2006), however, their methods were established under quite restrictive assumptions, such as prespecification of the number of faulty units and similar mean shift sizes in different faulty units. Besides its application to SPC, FDR control also can be used to identify important factors and effects in the analysis of two-level fractional factorial experiments (Tripolski Kimel, Benjamini, and Steinberg 2008).

In this article, we adopt the FDR control technique from microarray research to enhance the performance of SPC in multistage process monitoring and fault identification. The article is organized as follows. Section 2 describes several motivating examples with multistage processes, Section 3 presents the state-space model used to characterize the multistage process. Section 4 introduces the FDR control method to multistage processes. Sections 5 and 6 present and evaluate two SPC schemes, the FDR-adjusted Shewhart chart and the FDR-adjusted CUSUM chart. Section 7 revisits one of the motivating examples to demonstrate implementation of the newly proposed FDR-adjusted methods in a multistage process in practice. Finally, Section 8 provides a few concluding remarks and suggests future studies.

2. MOTIVATING EXAMPLES

Examples of multistage processes can be readily found in any modern manufacturing or service industry. Here we mention several from the recent literature that motivate our work.

An Example of Dielectric Layer Formation in the Semiconductor Industry

Kim and May (1999) investigated a typical multistage process in semiconductor manufacturing. They described a via formation process in multichip module dielectric layers composed of photosensitive benzocyclobutene. This process consists of several sequential stages, including spin coating, soft baking, exposing, developing, curing, and plasma descumming. At each stage, two quality characteristics—film thickness and the refractive index of the film—were measured. Kim and May (1999) constructed sequential neural network process models to characterize the multistage via formation process. There has been no subsequent study on monitoring and diagnosing such a process, however.

An Example of Semiconductor Photolithography in the Semiconductor Industry

Fenner, Jeong, and Lu (2005) investigated a multistage photolithography process in semiconductor manufacturing involving three main stages: spin-coating and baking the photoresist, exposing the photoresist, and developing the photoresist. Because of the proprietary nature of the third stage, only the first two stages were considered. The quality characteristics considered in the first stage were *relative unexposed photoactive compound concentration* ($M_{unexposed}$) and *resist thickness* (T). *Relative exposed photoactive compound concentration* ($M_{exposed}$) was considered in the second stage. The interstage relationship was described by the following linear regression models:

$$\begin{aligned} M_{unexposed} &= 0.91 + 1.61 \times 10^{-3} BTE - 2.10 \times 10^{-5} SPS, \\ T &= 1291.98 + 928.333(SPS)^{-1/2} \\ &\quad - 1.62 BTI - 19.49 BTE, \\ M_{exposed} &= M_{unexposed} - 0.000909 D + 0.0000112 T - 0.64, \end{aligned} \tag{1}$$

where BTE is the baking temperature, SPS is the spin speed, BTI is the baking time in seconds, and D is the exposure dose. The authors did not explore the monitoring and diagnosis of such a multistage process in semiconductor manufacturing, however.

An Example From Automobile Assembly

Lawless, MacKay, and Robinson (1999) and Agrawal, Lawless, and MacKay (1999) investigated four operational stages in installing car hoods in automobile assembly: hanging, painting, hardware, and finesse. Each stage contributed to the variance in the final flushness of the hood to the surrounding fenders. The relationships between these stages can be characterized by a state-space model (Xiang and Tsung 2008),

$$\begin{aligned} y_i &= x_i + v_i, \\ x_{i+1} &= \beta_i x_i + \omega_i \end{aligned} \tag{2}$$

for $i = 1, 2, 3, 4$ where x_i is the true flushness of the right rear at stage i and y_i is the measurement of the flushness. The model parameters in this example are $(\beta_1, \beta_2, \beta_3) = (1.15, 0.98, 1.06)$, and the standard deviations of $(\omega_1, \omega_2, \omega_3)$ are $(0.13, 0.11, 0.2)$. Again, the authors did not investigate how to monitor and diagnose such a process. The monitoring issue based on this model has been further explored by Xiang and Tsung (2008).

3. MODELING OF MULTISTAGE PROCESSES

We start by introducing the state-space model that can characterize a multistage process by incorporating physical laws and engineering knowledge. Extensive reviews of the state-space model have been provided by Basseville and Nikiforov (1993) and Shi (2007).

Suppose that the multistage process involves N stages and that $y_{n,j}$ is the quality measurement of the jth product observed at the nth operation stage, $n = 1, \ldots, N$ and $j = 1, 2, \ldots$. An in-control multistage process may be described by the following state-space model:

$$\begin{aligned} \mathbf{y}_{n,j} &= \mathbf{C}_n \mathbf{x}_{n,j} + v_{n,j}, \\ \mathbf{x}_{n,j} &= \mathbf{A}_n \mathbf{x}_{n-1,j} + \omega_{n,j}, \end{aligned} \tag{3}$$

where $\mathbf{x}_{n,j}$ denotes the quality information (e.g., part deviation) at stage n of product j, $\mathbf{A}_n$ is the dynamic matrix that denotes the transformation of the quality information from stage $n-1$ to stage n, and $\mathbf{C}_n$ is the observation matrix that relates the process states, $x_{n,j}$, to the quality measures, $\mathbf{y}_{n,j}$. Both $\mathbf{A}$ and $\mathbf{C}$ are assumed to be known constant matrixes at stage n, which may be derived from the process/product design information, physical laws, and engineering knowledge. In addition, ω signifies the unmodeled error, whereas v indicates the measurement error. Both ω and v follow independent multinormal distributions. Ding, Ceglarek, and Shi (2002) termed the first equation in (3) the state transition equation and the second the observation equation. In this article we follow the assumption considered by Xiang and Tsung (2008) and focus on the univariate case, where $\omega_{n,j} \sim \mathrm{N}(0, \sigma_{\omega_n})$, $v_{n,j} \sim \mathrm{N}(0, \sigma_v)$, and the initial state $x_0 \sim \mathrm{N}(a_0, \tau^2)$. a_0 and τ are usually assumed known in advance. Recent research related to the state-space model has been reported by Zhou, Huang, and Shi (2003), Huang and Shi (2004), and Ding et al. (2005).

An out-of-control condition with a fault in the current stage of operation (e.g., a fixture deviation) can be modeled with an additional term, $B_{n,j}U_{n,j}$, on the right side of the second equation of (3). Suppose that after the Jth product, a persistent mean shift of magnitude δ occurs at a certain stage, ζ, that is, $B_{n,j} = 1_{n=\zeta, j \geq J}$ and $U_{n,j} = \delta$. The out-of-control model can be written as

$$\begin{aligned} y_{n,j} &= C_n x_{n,j} + v_{n,j}, \\ x_{n,j} &= A_n x_{n-1,j} + \omega_{n,j} + 1_{n=\zeta, j \geq J} \delta. \end{aligned} \tag{4}$$

This out-of-control model is depicted in Figure 1.

According to Basseville and Nikiforov (1993), most change detection algorithms are based on generating "residuals" from the measurements that reflect the change in the process and then designing decision rules based on these residuals. Based on (3), the standardized one-step-ahead forecast error of $y_{n,j}$, given $y_{n-1,j}$, as written by Durbin and Koopman (2001), $e_{n,j}$, can be calculated from the following recursive method:

$$\begin{aligned} e_{n,j} &= v_{n,j} V_n^{-1/2}, \\ v_{n,j} &= y_{n,j} - C_n u_{n,j}, \\ u_{n,j} &= A_{n-1} u_{n-1,j} + G_{n-1,j} v_{n-1,j}, \\ V_n &= C_n^2 W_n + \sigma_v^2, \end{aligned} \tag{5}$$

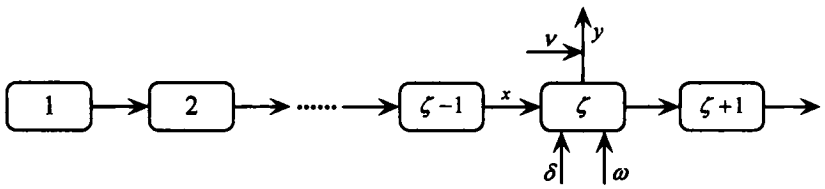

Figure 1. The mean shift in stage ζ in the state transition equation.

$$W_n = A_{n-1}^2 W_{n-1} - A_{n-1} C_{n-1} W_{n-1} G_{n-1} + \sigma_{\omega_n}^2,$$

$$G_n = A_n C_n W_n V_n^{-1},$$

where the initial values $v_{1,j} = y_{1,j} - C_1 A_1 a_0$, $e_{1,j} = v_{1,j}/V_1$, $u_{1,j} = 0$, $W_1 = \sigma_{\omega_1}^2 + A_1^2 \tau^2$. Durbin and Koopman (2001) showed that when the process is in control, $e_{n,j}$ is independently and identically distributed as a standard normal distribution, N(0, 1). When a particular stage, ζ, of the multistage process undergoes a change, as in (4), $e_{\zeta,j}$ will experience a mean shift while its variance remains the same. Thus the multistage process monitoring and diagnosis may be formulated into the following multiple hypotheses testing problem:

$$\begin{aligned} H_{0,n}: &\quad e_{nj} \sim \mathrm{N}(0, 1), \\ H_{1,n}: &\quad e_{nj} \sim \mathrm{N}(\mu_n, 1), \end{aligned} \tag{6}$$

$n = 1, \ldots, N$, where $\mu_n \neq 0$.

Most multiple hypotheses testing methods applied to multistage process monitoring aim to control the type I error rate. But the power of such methods becomes unsatisfactorily low when the number of hypotheses is large. To handle the high-dimensional problem that will surely surface in a multistage process, we apply the FDR control approach, which controls the proportion of wrong rejections among all the rejections. We introduce this method in the next section.

4. FALSE DISCOVERY RATE CONTROL METHODS

The conventional approach to multiple hypotheses testing is to control the risk of a type I error occurring. The Bonferroni and sequential Bonferroni methods are examples of methods that take this approach. But multiple statistical tests aimed at controlling the type I error rate have a serious drawback in terms of reduced detection power. Trying to minimize the risk of even a single type I error will lead to an unacceptably low detection power for each test.

From the pioneering work of Benjamini and Hochberg (1995), the FDR is the expected proportion of false-positive findings among all rejected hypotheses. The FDR control method aims to control the FDR instead of the type I error rate. The FDR control method has much higher power when a large number hypotheses are being tested. The more hypotheses there are, the more significant the superiority of this method. When none of the hypotheses is false, controlling the FDR is equivalent to controlling the type I error rate.

Suppose that a multistage process involves a total of N stages. N_0 stages remain in control while $N_1 = N - N_0$ stages go out of control. Table 1 shows the possible outcomes of the multiple hypotheses testing. A false discovery, as defined by Benjamini and Hochberg (1995), is an in-control stage that is incorrectly identified as a faulty stage. Suppose that the number of false discoveries is B and that the total number of the stages that are identified as faulty stages is R. Then the FDR is defined as

$$FDR = E\left(\frac{B}{R} \,\middle|\, R > 0\right) \Pr(R > 0), \tag{7}$$

the proportion of the false discoveries among all discoveries.

Average power is used extensively in statistics to evaluate the detection capability of multiple hypotheses testing methods. Average power is defined as

$$\text{Average power} = E\left(\frac{F}{N_1}\right) \Pr(N_1 > 0), \tag{8}$$

where F is the number of faulty stages identified correctly. Marshall et al. (2004) and others call average power the successful detection rate (SDR). Obviously, a desirable multiple hypotheses testing method requires both a low FDR and high average power.

Benjamini and Hochberg (1995) proposed a simple linear step-up procedure aimed at controlling the FDR at a prespecified level, α, while maximizing the number of rejected hypotheses. For m independent tests, $H_1, H_2, \ldots, H_m$, let $p_1, p_2, \ldots, p_m$ be their p-values. The simple linear step-up procedure is as follows:

1. Rank the p-values in ascending order, $p_{(1)} \leq p_{(2)} \leq \cdots \leq p_{(m)}$.
2. $l = \max\{j : p_{(j)} \leq j\alpha/m,\ 1 \leq j \leq m\}$.
3. If $l > 0$, then reject all the hypotheses associated with $p_{(1)}, \ldots, p_{(l)}$. Otherwise, do not reject any hypotheses.

Benjamini and Hochberg (1995) proved that this simple linear step-up procedure guarantees

$$E(FDR) \leq \frac{m_0}{m}\alpha \leq \alpha,$$

where m_0 is the number of true null hypotheses. When all of the null hypotheses are true, namely $m_0 = m$, the simple linear step-up method can strictly control the FDR at level α. If some alternative hypotheses are true, then the simple linear step-up method may be somewhat conservative; however, if the value

Table 1. Possible outcomes of multiple hypotheses testing

	Identified as in-control stages	Identified as faulty stages	Total
In-control stages	A	B	N_0
Faulty stages	E	F	N_1
Total	M	R	N

of m_0 is available, we can still strictly control the FDR exactly at α, which can lead to a higher average power. To further improve the power of the simple linear step-up method, Benjamini, Krieger, and Yekutieli (2006) incorporated the adaptive estimation of m_0 into a two-stage linear step-up procedure, as follows:

1. Use the linear step-up procedure at level $\alpha' = \alpha/(1+\alpha)$. Let r_1 be the number of rejected hypotheses. If $r_1 = 0$ does not reject any hypothesis, stop; if $r_1 = m$ rejects all m hypotheses, stop.
2. Let $\hat{m}_0 = m - r_1$.
3. Use the linear step-up procedure with $\alpha^* = \alpha' m/\hat{m}_0$.

Obviously, the closer the ratio, m_0/m, is to 0, the more significant the increase in average power.

Benjamini and Hochberg (1995) and Benjamini, Krieger, and Yekutieli (2006) proved that when all m tests are independent, the simple and two-stage linear step-up procedures can guarantee FDR control. Otherwise, as Benjamini and Yekutieli (2001) showed, despite the dependent structure of the hypotheses, the simple linear step-up procedure conducted with $\alpha/\sum_{i=1}^{m} 1/i$ in place of α can still control FDR at a level less than or equal to $m_0\alpha/m$.

Because FDR control guarantees a higher average power, in what follows we discuss how to implement FDR control in multistage process monitoring and diagnosis.

5. THE FALSE DISCOVERY RATE–ADJUSTED SHEWHART CHART

To apply the FDR control method to multistage process monitoring and diagnosis, we first consider an FDR-adjusted Shewhart chart (Shewhart 1931) based on the two-stage linear step-up procedure. We do this because the Shewhart chart is among the most popular control schemes for process monitoring. Suppose that there are N stages in a multistage process that can be described by a state-space model as in (3), and that all of the parameters in the model are assumed to be known. Let $e_{n,j}$ denote the standardized one-step-ahead forecast error of stage n of product j, then $\{e_{n,j}, n = 1, 2, \ldots, N\}$ is iid random noise that follows $N(\mu_n, 1)$. Note that when the process is in control, $\mu_n = 0$.

To test the hypotheses as in (6), we establish multiple control charts based on FDR control methods. Alternatively, we also construct multiple control charts based on the conventional type I error rate control method for benchmarking.

Because the standardized one-step-ahead forecast errors follow standard normal distributions when the process is in control, the p-value of the control statistics of each control chart can be readily calculated as

$$p_{n,j} = 2\big(1 - \Phi(|e_{n,j}|)\big), \qquad n = 1, \ldots, N, \tag{9}$$

where Φ is the distribution function of the standard normal distribution.

The FDR-adjusted Shewhart chart can be easily established given the p-values of each stage and the independence between $e_{n,j}$. Suppose that $\{p_{(n),j}, n = 1, \ldots, N\}$ are the p-values in ascending order and that the signaling time of the FDR-adjusted Shewhart chart, T, is

$$\begin{aligned} l &= \max\big\{n : p_{(n),j} \le n\alpha/N, 1 \le n \le N\big\}, \\ T &= \inf\{j : l \ge 1\}. \end{aligned} \tag{10}$$

Suppose that the FDR-adjusted Shewhart chart gives an alarm at product J. All of the stages associated with $p_{(1),J}, \ldots, p_{(l),J}$ are viewed as faulty stages. The step-by-step procedure for using an FDR-adjusted Shewhart chart is as follows:

1. Model a multistage process with N stages by a state-space model as in (3), assuming that all of the parameters in the model are known.
2. Choose the in-control average run length (ARL) of the FDR-adjusted Shewhart chart, ARL_0. The value of α can be determined later.
3. For product j, calculate the standardized one-step-ahead forecast error of each stage, $e_{1,j}, e_{2,j}, \ldots, e_{N,j}$, by (5).
4. Calculate $p_{(1),j}, \ldots, p_{(N),j}$, the ascending ordered p-values of $e_{1,j}, e_{2,j}, \ldots, e_{N,j}$, by (9).
5. Find the largest l using the two-stage linear step-up procedure because of the independency of $e_{1,j}, e_{2,j}, \ldots, e_{N,j}$.
6. If $l > 0$, the process is determined to be out of control. Those stages associated with $p_{(1),j}, \ldots, p_{(l),j}$ are identified as faulty stages. Otherwise, continue to sample. For product $j+1$, reiterate steps 3–6.

Alternatively, conventional multiple Shewhart charts based on type I error rate control can be established, for which the signaling time, T_h, is

$$T_h = \inf\{j, |e_{n,j}| \ge h, n = 1, 2, \ldots, N\}, \tag{11}$$

where h is the control limit that can be determined by the overall type I error rate. The stages with $|e_{n,j}| \ge h$ are diagnosed as faulty stages. The step-by-step procedure for constructing the multiple Shewhart charts is as follows:

1. Model a multistage process with N stages by a state-space model as in (3), assuming that all of the parameters in the model are known.
2. Choose the in-control ARL of the multiple Shewhart charts, ARL_0; the value of h can be determined later.
3. For product j, calculate the standardized one-step-ahead forecast error of each stage, $e_{1,j}, e_{2,j}, \ldots, e_{N,j}$, by (5).
4. If any $|e_{n,j}| \ge h, n = 1, 2, \ldots, N$, the process is determined to be out of control. Those stages with $|e_{n,j}|$ larger than or equal to h are identified as faulty stages. Otherwise, continue to sample. For product $j+1$, reiterate steps 3–4.

In he next section, we provide numerical comparisons between the FDR-adjusted Shewhart chart and the multiple Shewhart charts.

5.1 Fault Identification Performance Evaluation

In this section we compare the performance of the multiple Shewhart charts based on type I error rate control and the FDR-adjusted Shewhart chart. Suppose that a multistage

Table 2. Comparison of the FDR-adjusted Shewhart chart and the multiple Shewhart charts. Equal mean shift magnitude. $N = 30$, in-control $ARL = 700$. Values in parentheses are for the multiple Shewhart charts

	Number of out-of-control stages								
	1			3			6		
δ	*ARL*	Power (%)	FDR (%)	*ARL*	Power (%)	FDR (%)	*ARL*	Power (%)	FDR (%)
0.50	671 (671)	6.7 (6.7)	0.12 (0.12)	582 (582)	7.8 (7.8)	0.13 (0.13)	464 (465)	7.6 (7.6)	0.12 (0.12)
1.00	591 (590)	17.6 (17.5)	0.12 (0.12)	310 (310)	19.5 (19.5)	0.13 (0.13)	160 (160)	13.5 (13.4)	0.12 (0.12)
1.50	420 (419)	40.5 (40.4)	0.13 (0.13)	107 (107)	28.5 (28.4)	0.14 (0.14)	42.1 (42.2)	16.1 (15.9)	0.13 (0.13)
2.00	242 (242)	62.5 (61.5)	0.16 (0.16)	34.5 (34.6)	32.2 (31.8)	0.16 (0.15)	11.8 (11.9)	17.7 (16.9)	0.18 (0.17)
3.00	59.9 (59.9)	88.7 (88.6)	0.25 (0.20)	5.1 (5.2)	36.6 (34.8)	0.26 (0.23)	2.0 (2.1)	25.3 (21.2)	0.19 (0.23)
4.00	15.4 (15.4)	97.0 (96.7)	0.49 (0.22)	1.7 (1.7)	45.4 (41.3)	0.55 (0.46)	1.0 (1.1)	48.4 (37.8)	0.56 (0.30)
5.00	5.4 (5.4)	98.6 (98.5)	0.90 (0.35)	1.1 (1.1)	62.0 (55.9)	0.98 (0.60)	1.0 (1.0)	77.3 (66.2)	0.97 (0.37)

process involves $N = 30$ operation stages. Assume that the correlation among the process stages can be described by a simple state-space model with identity constants, A_n and C_n, in (3). (We discuss the effect of process parameters A_n and C_n in the next section.) The other parameters in the state-space model are $\sigma_v = 1$, $\sigma_{\omega_n} = 1$, and, for the initial state, $a_0 = 0$ and $\tau = 1$.

The in-control ARL of the two types of Shewhart charts is fixed at 700. Two types of out-of-control scenarios are considered. In the first scenario, all of the faulty stages experience mean shifts of the same magnitude. One, 3, or 6 out of 30 stages in the process are randomly chosen as faulty stages. The common mean shifts in the faulty stages considered are 0.5, 1.0, 1.5, 2.0, 3.0, 4.0, and 5.0. As for the second scenario, 3 or 6 out of 30 stages are randomly chosen to be out-of-control stages. The faulty stages are grouped into three groups of equal size. In category I, mean shift magnitudes of the three groups of faulty stages are 0.5, 1.0, and 1.5. In category II, these mean shift magnitudes are 0.5, 1.5, and 2.5, and in category III, they vary in an even wider range, 0.5, 2.0, and 3.5.

Tables 2 and 3 compare the two scenarios in terms of out-of-control ARL, average power, and FDR. Values corresponding to the multiple Shewhart charts are given in parentheses. The results were obtained from 1,000,000 Monte Carlo simulation runs. As shown in these two tables, the out-of-control ARLs of the two types of charts are approximately the same. Both have an FDR of <1%, which is quite satisfactory. In Table 2, when the number of faulty stages is only one, the two methods perform similarly. Both methods also have quite satisfactory average power; for example, when $\delta = 4.0$, the probability of correctly identifying the out-of-control stage exceeds 96%. But the average power of both methods decreases as the number of faulty stages increases; for instance, when the first three stages go out of control and δ is 4.0, the average power of the FDR-adjusted Shewhart chart drops from 100% to 45%, and the performance of the multiple Shewhart charts deteriorates more seriously, to 41%. When the number of faulty stages increases to six, the average power of the FDR-adjusted Shewhart chart is 48%, whereas that of the multiple Shewhart charts is only 38%. For mean shifts < 2.0, the two methods have similar average power.

In Table 3, due to the inequality of the mean shift magnitude, the average power of both methods seriously deteriorates. The underlying reason is that rapid detection of large mean shifts hinders the detection of smaller mean shifts. But when the number of faulty stages is large, the average power of the FDR-adjusted Shewhart chart still exceeds that of the multiple Shewhart charts; for instance, when the first six stages go out of control with category III mean shifts, the average power of the FDR-adjusted Shewhart chart is about 34%, whereas that of the multiple Shewhart charts is about 27%.

The numerical results are influenced only slightly for other possible choices of faulty stages; however, the FDR-adjusted Shewhart chart always maintains its superiority.

In summary, the FDR-adjusted Shewhart chart has higher average power than the multiple Shewhart charts under two out-of-control scenarios. We next discuss other FDR-adjusted control charts that could further improve the performance of the FDR-adjusted Shewhart chart.

5.2 The Effect of Process Parameters *A* and *C*

In this section we exlore the effect of the process parameters (A_n, C_n) on the performance of the multiple Shewhart charts

Table 3. Comparison of the FDR-adjusted Shewhart chart and the multiple Shewhart charts. Varying mean shift magnitude. $N = 30$, in-control $ARL = 700$. Values in parentheses are for the multiple Shewhart charts

	Number of out-of-control stages					
	3			6		
δ	*ARL*	Power (%)	FDR (%)	*ARL*	Power (%)	FDR (%)
Category I	106.4 (106.5)	29.49 (29.32)	0.12 (0.11)	41.8 (42.0)	16.05 (15.78)	0.15 (0.15)
Category II	12.4 (12.5)	34.64 (33.72)	0.11 (0.11)	4.3 (4.4)	20.07 (18.32)	0.18 (0.16)
Category III	2.7 (2.7)	40.60 (37.69)	0.10 (0.07)	1.3 (1.3)	33.89 (27.01)	0.35 (0.22)

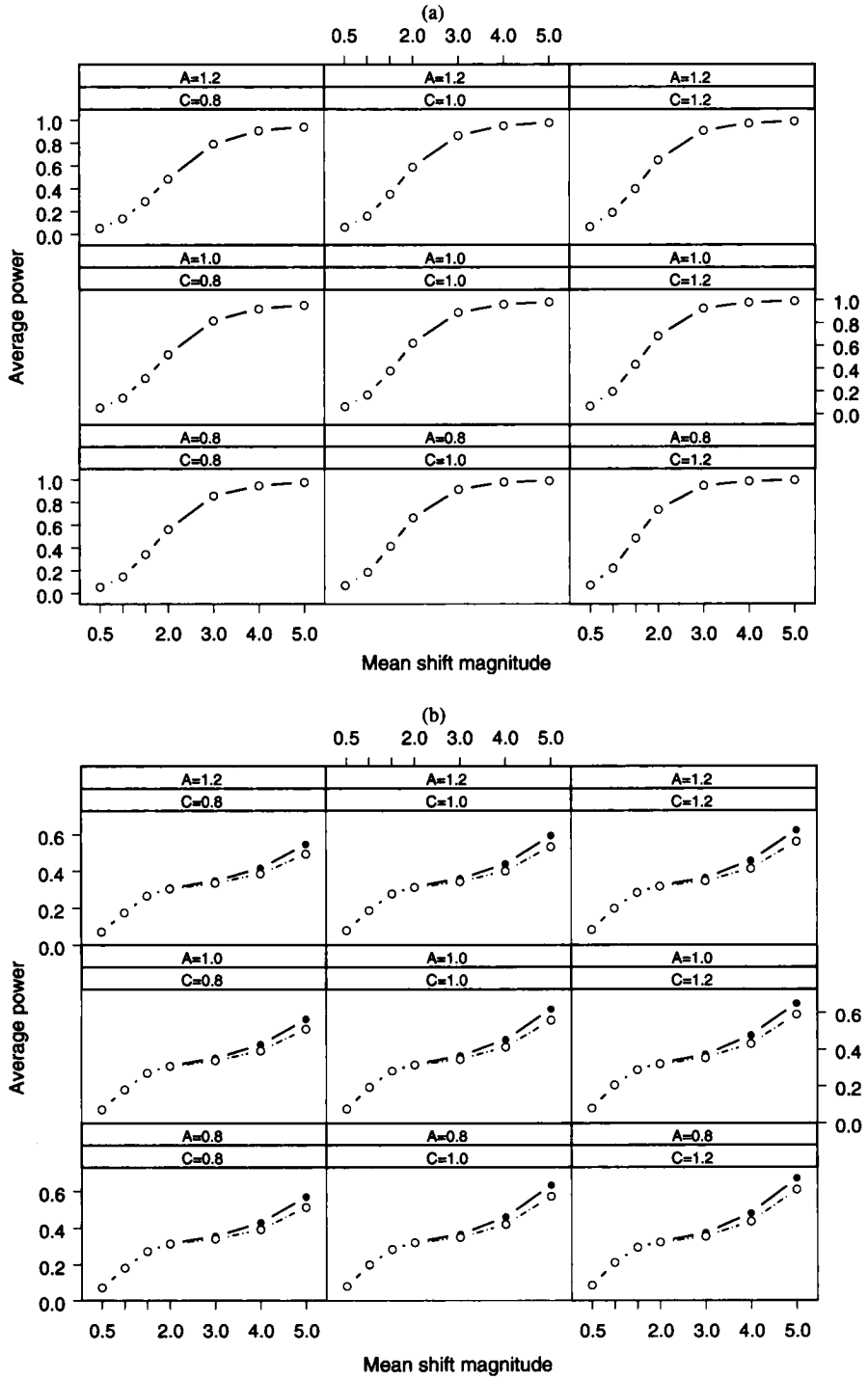

Figure 2. Average power of the FDR-adjusted Shewhart chart (solid lines with solid circles) and the multiple Shewhart charts (dashed lines with empty circles) with varying process parameters, A_n and C_n. The mean shifts of the different stages are equal. (a) Number of faulty stages = 1. (b) Number of faulty stages = 3. (c) Number of faulty stages = 6.

based on FDR control and type I error rate control. Suppose that there are $N = 30$ stages in a multistage process and that the in-control ARL is also fixed at 700. The values of A_n and C_n are assumed to be known and to vary from 0.8 to 1.0 and 1.2. Other parameters in the state-space model are kept constant, $\sigma_v = 1$, $\sigma_{\omega_n} = 1$, $a_0 = 0$, and $\tau = 1$.

Comparisons of the the FDR-adjusted Shewhart chart and the multiple Shewhart charts are shown graphically in Figures 2 and 3. Figure 2 illustrates the average power of the two methods when the first one, three, or six stages in the process are faulty stages with equal shifts in magnitude. Figure 3 depicts the average power of the two methods with varying mean shifts. The simulation results also demonstrate that both methods nearly have the same FDR and out-of-control ARL regardless of the variation in A_n and C_n.

In Figure 2, when only the first stage of the process goes out of control, the average power of the two control schemes is quite close. The superiority of the FDR-adjusted Shewhart

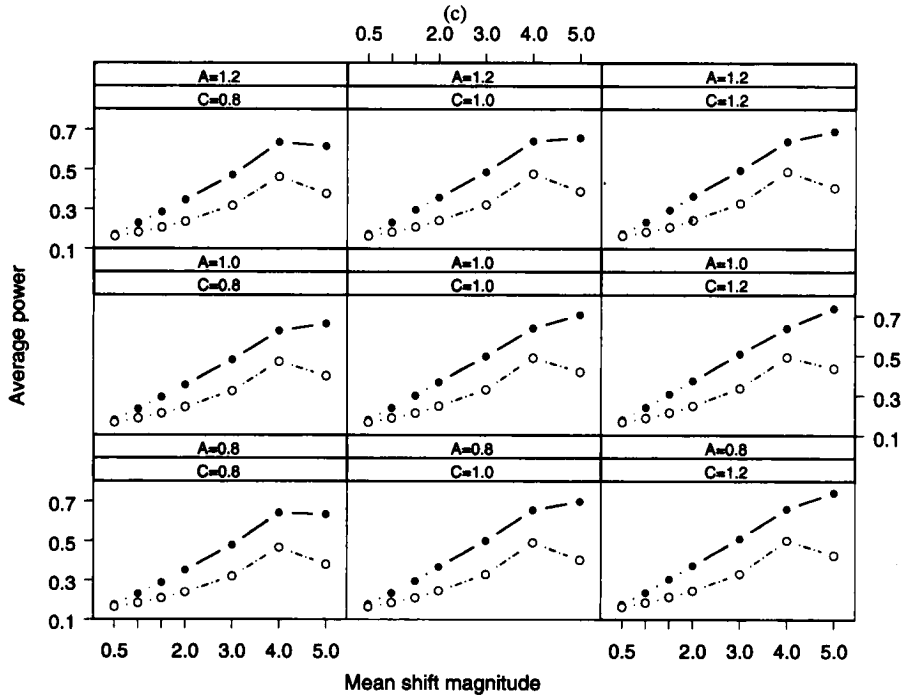

Figure 2. (Continued.)

chart becomes more obvious when the number of faulty stages increases. For instance, when the first six stages experience a mean shift of magnitude five, the average power of the FDR-adjusted Shewhart chart exceeds that of the multiple Shewhart charts by approximately 10%.

Panels (a)–(c) in Figure 3 show that when the difference between the varying mean shifts is small, say 0.5, the superiority of the FDR-adjusted Shewhart chart is marginal. As the difference between mean shifts increases, the average power of the FDR-adjusted Shewhart chart becomes more obvious; for example, when category III mean shifts occur in the first six stages, the average power of the FDR-adjusted Shewhart chart is about 5% higher than that of the multiple Shewhart charts.

In summary, when A_n and C_n vary within a certain range, the FDR-adjusted Shewhart chart and the multiple Shewhart

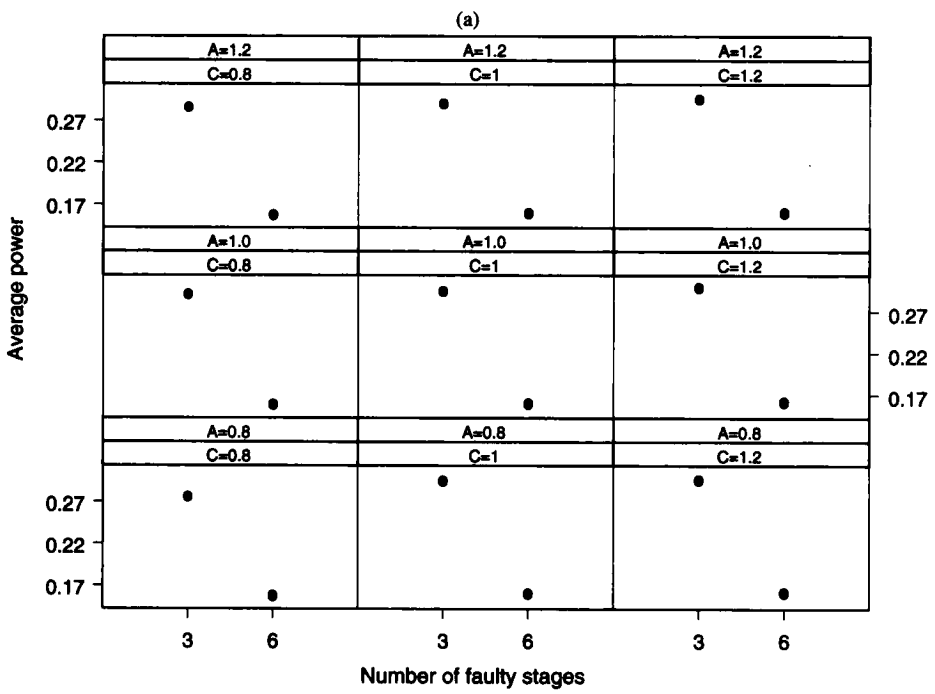

Figure 3. Average power of the FDR-adjusted Shewhart chart (solid dots) and the multiple Shewhart charts (circles) with varying process parameters, A_n and C_n and varying mean shifts. (a) Category I mean shifts. (b) Category II mean shifts. (c) Category III mean shifts.

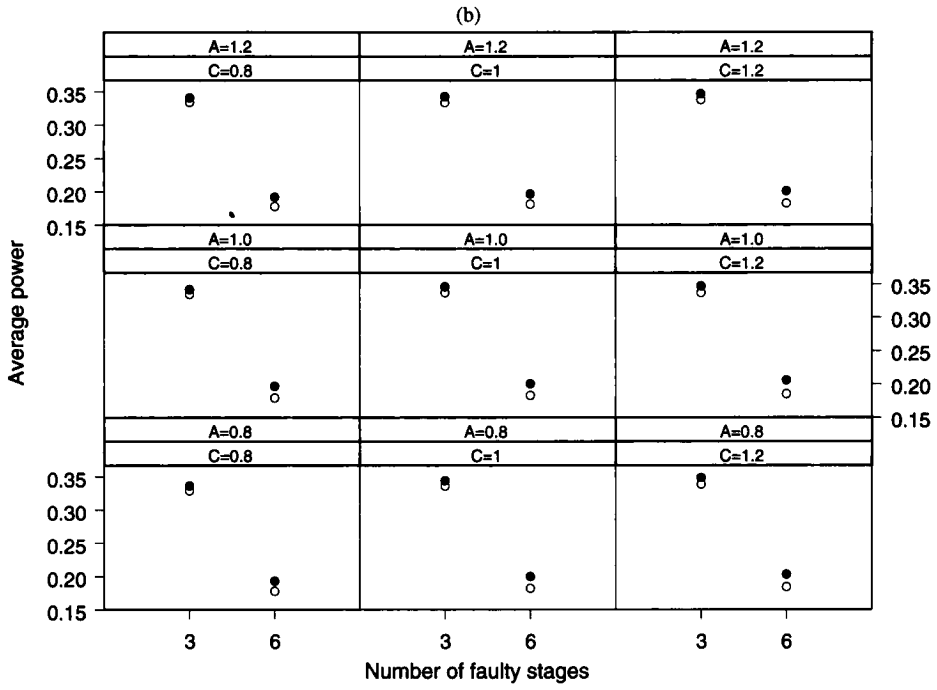

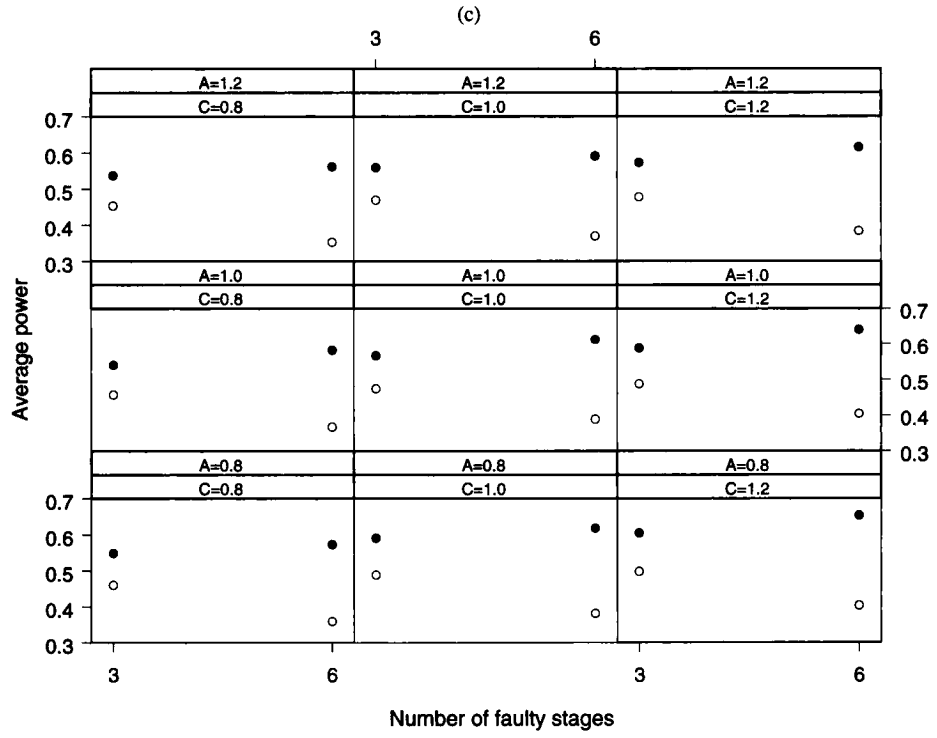

Figure 3. (Continued.)

charts have nearly the same average power; however, the FDR-adjusted Shewhart chart is always superior.

6. FALSE DISCOVERY RATE–ADJUSTED CUSUM CHART

Along with Shewhart-type charts, the CUSUM chart is popular and has proven optimal properties for a given size of mean shift (Bagshaw and Johnson 1975). It is well known that the Shewhart-type charts are generally good at detecting large mean shifts, whereas the CUSUM chart is more proficient in detecting small but persistent mean shifts. Hawkins (1991, 1993) suggested using the CUSUM chart for each variable in a cascading process, such as a multistage process. In this section we investigate applying multiple CUSUM charts based on FDR control to a multistage process for fault identification.

Suppose that the total number of stages in a multistage process is N. Let $e_{n,j}$ be the standardized one-step-ahead forecast error of the nth stage of product j, which is random noise from a standard normal distribution if the process is in control.

To detect a change as in (4), we establish a two-sided CUSUM chart on $e_{n,j}$ for each stage. The two-sided CUSUM chart for the nth stage for product j is defined as follows:

$$\begin{aligned} S_{n,j}^{+} &= \max\{0, S_{n,j-1}^{+} + e_{n,j} - k\}, \\ S_{n,j}^{-} &= \max\{0, S_{n,j-1}^{-} - e_{n,j} - k\}, \end{aligned} \tag{12}$$

where $k > 0$ is the reference value. For large values of $S_{n,j}^{+}$, the CUSUM statistic can be rewritten as

$$S_{n,j}^{+} = S_{n,j-1}^{+} + e_{n,j} - k. \tag{13}$$

Similarly, $S_{n,j}^{-}$ can be simplified as

$$S_{n,j}^{+} = S_{n,j-1}^{+} - e_{n,j} - k. \tag{14}$$

Each stage in a multistage process has two control statistics. $S_{n,j}^{+}$ is used to detect positive mean shifts, whereas $S_{n,j}^{-}$ is used to detect negative mean shifts. When the process is in control, $S_{n,j}^{+}$ and $S_{n,j}^{-}$ share the same distribution function, Ψ.

Once the distribution function, Ψ, is obtained, the p-values of the CUSUM statistics of the jth product at the nth stage, $p_{n,j}^{+} = 1 - \Psi(S_{n,j}^{+})$ and $p_{n,j}^{-} = 1 - \Psi(S_{n,j}^{-})$, can be calculated. Because there are N stages in the process, we have a total of N pairs of p-values. Based on these p-values, the FDR-adjusted CUSUM chart can be established as follows:

1. Model a multistage process with N stages with a state-space model as in (3), assuming that all of the parameters in the model are known.
2. Choose the in-control ARL of the FDR-adjusted CUSUM chart, ARL_0. The value of the FDR, α, can be determined later.
3. For product j, calculate the standardized one-step-ahead forecast error of each stage, $e_{1,j}, e_{2,j}, \ldots, e_{N,j}$ by (5).
4. Establish a two-sided CUSUM chart with reference value k for each stage; calculate $S_{1,j}^{+}, S_{n,j}^{-}, S_{1,j}^{+}, S_{2,j}^{-}, \ldots, S_{N,j}^{+}$, $S_{N,j}^{-}$, based on (12).
5. Calculate $\{p_{n,j}^{+}$ and $p_{n,j}^{-}, n = 1, 2, \ldots, N\}$, the p-values of $S_{n,j}^{+}$ and $S_{n,j}^{-}$.
6. Order the p-values $\{p_{n,j}^{+}$ and $p_{n,j}^{-}, n = 1, 2, \ldots, N\}$ as $p_{(1)}, p_{(2)}, \ldots, p_{(2N)}$ in ascending order.
7. Find the largest l by using the simple linear step-up procedure. $\alpha / \sum_{i=1}^{2N} \frac{1}{i}$ is used in place of α.
8. If $l > 0$, the process is determined to be out of control. All of the stages associated with $\{p_{(n),j}, n = 1, 2, \ldots, l\}$ are diagnosed as faulty stages. Otherwise, continue to sample. For product $j + 1$, reiterate steps 3–8.

In contrast, the stopping time of the conventional multiple CUSUM charts, T_h, given reference value k and control limit h, is calculated as

$$\begin{aligned} T_h^{+}(k) &= \inf\{j : S_{n,j}^{+} \geq h,\ n = 1, 2, \ldots, N\}, \\ T_h^{-}(k) &= \inf\{j : S_{n,j}^{-} \geq h,\ n = 1, 2, \ldots, N\}, \\ T_h(k) &= \min(T_h^{+}(k), T_h^{-}(k)). \end{aligned} \tag{15}$$

The multiple CUSUM charts are implemented as follows:

1. Model a multistage process with N stages with a state-space model as in (3), assuming that all of the parameters in the model are known.
2. Choose the in-control ARL of the multiple CUSUM charts, ARL_0. The value of control limit, h, can be determined later.
3. For product j, calculate the standardized one-step-ahead forecast error of each stage, $e_{1,j}, e_{2,j}, \ldots, e_{N,j}$ by (5).
4. Establish a two-sided CUSUM chart with reference value k for each stage; calculate $S_{1,j}^{+}, S_{n,j}^{-}, S_{1,j}^{+}, S_{2,j}^{-}, \ldots, S_{N,j}^{+}$, $S_{N,j}^{-}$, based on (12).
5. For each stage, check whether $S_{n,j}^{+} \geq h$ or $S_{n,j}^{-} \geq h$; if yes, then such stages are diagnosed as faulty stages and the process is considered out of control. Otherwise, continue to sample. For product $j + 1$, reiterate steps 3–5.

A critical step in applying the FDR control method to the CUSUM chart step is to calculate the p-values of the CUSUM control statistics, $S_{n,j}^{+}$ and $S_{n,j}^{-}$. Here we provide three methods for approximating $\Pr(S_{n,j}^{+} \geq x)$ and $\Pr(S_{n,j}^{-} \geq x)$. The first method is based on Markov chain theory, whereas the other two methods are based on Brownian motion with drift. Because $S_{n,j}^{+}$ and $S_{n,j}^{-}$ share the same distribution when the process is in control, we use $S_{n,j}^{+}$ for explanatory purposes.

6.1 Approximation Based on Markov Chain Theory

When a multistage process is well under control, the standardized one-step-ahead forecast errors of all of the stages are iid as a standard normal distribution. Therefore, the CUSUM charts based on the residuals of different stages also are iid. Thus we need only study the distribution of the control statistics of one typical stage, n, in the process.

It has been widely accepted that the ARL of the CUSUM chart can be calculated by the Markov chain method (Brook and Evans 1972). Likewise, the Markov chain method also can be used to approximate the limiting distribution of the CUSUM statistics. The control statistics of the CUSUM chart, $S_{n,j}^{+}$ and $S_{n,j}^{-}$, can be viewed as discrete-time Markov chains whose state spaces contain all of the nonnegative real numbers. The future state, $S_{n,j+1}^{+}$, given the past states, $S_{n,j-1}^{+}, \ldots, S_{n,0}^{+}$, and the present state, $S_{n,j}^{+}$, is independent of the past states and depends only on the present state, as does $S_{n,j+1}^{-}$.

We describe the approximation method based on Markov chain theory in detail in Appendix A. In brief, suppose that the state space of $S_{n,j}^{+}$ can be discretized into $r + 1$ subintervals, $\{E_0, E_1, \ldots, E_r\}$. Then the limiting distribution of the discretized Markov chain with finite states, $\{\pi_i, i = 0, 1, \ldots, r\}$, can be calculated, where π_i is the probability that $S_{n,j}^{+}$ falls into subinterval E_i. As r increases, the length of each subinterval decreases, and the limiting distribution of the discretized Markov chain moves closer to the true limiting distribution of $S_{n,j}^{+}$. When r is large enough, the p-value of the CUSUM statistic can be computed. Obviously, $\Pr(S_{n,j}^{+} \geq 0) = 1$. For $x > 0$,

$$\begin{aligned} \Pr(S_{n,j}^{+} \geq x) &= \sum_{i=a}^{r} \pi_i, \\ a &= \{l : x \in E_l,\ l = 0, 1, \ldots, r\}. \end{aligned} \tag{16}$$

The p-values of the CUSUM statistics can be approximated based on the foregoing formula.

6.2 Approximation Based on Brownian Motion Theory

An easier alternative method for approximating the p-values is based on the theory of Brownian motion with drift. Because the standardized one-step-ahead forecast error, $e_{n,j}$, of a typical stage, n, of a multistage process follows a standard normal distribution, $e_{n,1} - k, e_{n,2} - k, \ldots, e_{n,j} - k$ are independently identically and normally distributed with $E(e_{n,j} - k) < \infty$. When the value of the CUSUM statistics is very large, the formula for calculating the CUSUM statistics can be simplified as $S^+_{n,j} = S^+_{n,j-1} + e_{n,j} - k$. Then $\{S^+_{n,j}\}$ can be viewed as Brownian motion with a drift coefficient $-k$ (Ross 1996).

Suppose that $X(t)$ is Brownian motion with drift μ. Based on the theory of Brownian motion, provided that $A, B > 0$, the probability that the process hits A before $-B$ when the process starts at $x\,(-B < x < A)$ is

$$\Pr\big(X(t) \text{ hits } A \text{ before } -B | X(0) = x\big) \approx \frac{e^{2\mu B} - e^{2\mu x}}{e^{2\mu B} - e^{-2\mu A}}. \quad (17)$$

Suppose that the Brownian motion with drift starts with 0. Then the foregoing probability can be simplified as

$$\Pr\big(X(t) \text{ hits } A \text{ before } -B | X(0) = 0\big) \approx \frac{e^{2\mu B} - 1}{e^{2\mu B} - e^{-2\mu A}}. \quad (18)$$

Provided that $\mu < 0$ and letting B approach infinity, we can obtain

$$\Pr(X(t) \text{ hits } A | X(0) = 0) \approx e^{2\mu A}. \quad (19)$$

Because the drift coefficient of $S^+_{n,j}$ is $-k < 0$, using the theory of Brownian motion, the probability $\Pr(S^+_{n,j} \geq x)$ can be approximated by

$$\Pr(S^+_{n,j} \geq x | S^+_{n,0} = 0) \approx e^{-2kx} \quad \text{for } x > 0. \quad (20)$$

Although the foregoing approximation is simple enough, it may not be used directly. Because the CUSUM chart is actually a discrete time Markov chain while Brownian motion evolves continuously, there is a discrepancy between the actual value of the p-value of the CUSUM statistic and the approximate value as in (20). To compensate for the discrepancy, Siegmund (1985) provided a revised approximation of expression (20) that gives greater accuracy. Here we use Siegmund's result with some modification to get a better approximation of the p-value of the CUSUM statistic. The corrected approximation of the p-value of the CUSUM statistic (hereinafter referred to as the corrected Brownian motion method) is as follows:

$$\Pr(S^+_{n,j} \geq x) \approx e^{-2k(x+\rho)} \quad \text{for } x > 0, \quad (21)$$

where ρ is a constant that equals 0.583. The derivation of (21) is presented in Appendix B.

6.3 Evaluation of Different Approximation Methods

So far, we have described three methods of approximating the p-values of the CUSUM statistics: one method based on Markov chain theory and two methods based on Brownian motion models. To evaluate these three methods, we use the empirical distribution of the CUSUM statistics as a benchmark. We assume that a CUSUM chart reaches its steady state after 10,000 observations; therefore, the 10,001st CUSUM statistic is collected. A total of 1 million such CUSUM statistics are collected to get the empirical distribution.

Figure 4 shows the p-values of the CUSUM chart with reference value 0.5 obtained using the three approximation methods and the empirical distribution. The approximate values based on the corrected Brownian motion method and the Markov chain method are much closer to the values obtained by the empirical distribution. As the value of the CUSUM statistic increases, the p-values obtained by four methods gradually converge.

To quantitatively evaluate the three approximation methods, M equally spaced points are drawn from the state space of the CUSUM statistic. The p-value obtained via the empirical distribution at point i is designated p_i^E, and the p-values approximated are designated p_i^{App}. The mean squared error (MSE) of the approximation method, defined as

$$MSE_{App} = \frac{1}{M}\sum_{i=1}^{M}(p_i^E - p_i^{App})^2, \quad (22)$$

is used as a metric. For example, the MSE of the approximation based on Markov chain theory is $\frac{1}{M}\sum_{i=1}^{M}(p_i^E - p_i^M)^2$, where p_i^M is the p-value obtained by the Markov chain method at point i. Obviously, the smaller the MSE, the better the approximation method.

For the CUSUM chart with reference value 0.5, the MSE of the approximate p-values obtained from the three methods are 3×10^{-7} for the Markov chain method, 8×10^{-2} for the Brownian motion method, and 8×10^{-4} for the corrected Brownian motion method. To save space, the MSEs for CUSUM charts with different reference values are not shown. Comparing the MSEs shows that the approximation method based on Markov chain theory has the greatest accuracy. But this method is also more computationally demanding and may not be feasible in practice. In the next section we present a performance comparison of the FDR-adjusted CUSUM chart based on three types of approximation methods demonstrating that the FDR-adjusted CUSUM chart is actually quite robust to approximation errors.

6.4 Fault Identification Performance Evaluation

Tables 4–9 compare the multiple CUSUM charts based on FDR control and type I error rate control in terms of out-of-control ARL, average power, and FDR. The results were obtained through 1 million Monte Carlo simulation runs. Here $k = 0.5$ for demonstration purposes. The common in-control ARL is 700, and the number of stages, N, is 30. To save space, the tables do not provide the simulation results for other choices of N. The process parameters of the state-space model are the same as those reported in Section 5.2.

From Tables 4–9, we can see that although the three types of approximation methods vary, the FDR-adjusted CUSUM chart is quite robust to the approximation methods; that is, the FDR-adjusted CUSUM chart based on the three approximation methods has nearly the same performance. Therefore, if computational effort is a concern, then the corrected Brownian motion method is recommended.

Similar to the results shown in Tables 2 and 3, the out-of-control ARLs of multiple CUSUM charts and the FDR-adjusted CUSUM chart remain nearly the same. The FDRs are all under good control.

Comparing Tables 2 and 3 and Tables 4–9, the average power is significantly improved in the latter, because the CUSUM

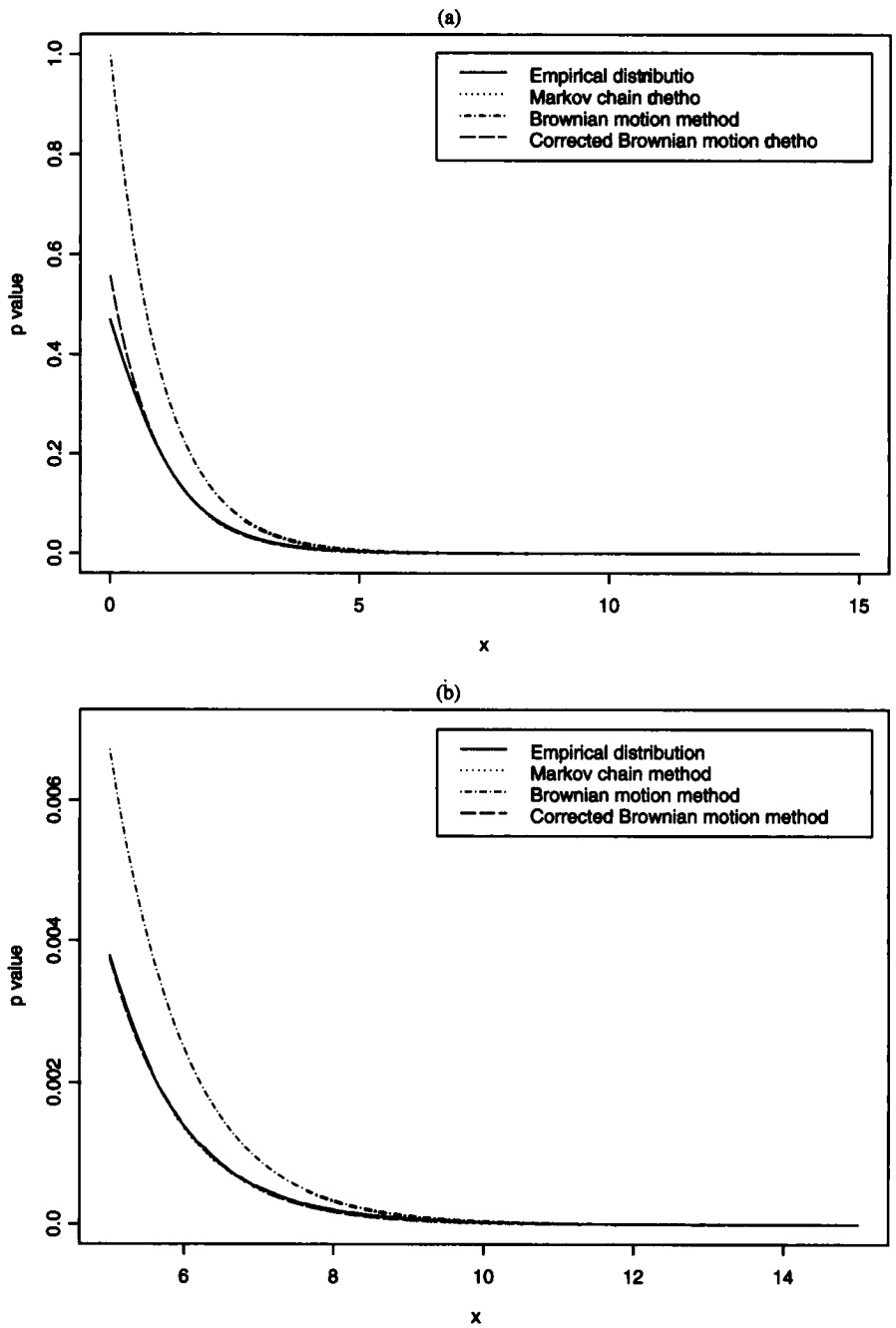

Figure 4. Comparison of methods for approximating the p-values of the CUSUM statistics ($k = 0.5$). (a) An overview. (b) Enlarged view of the right end.

Table 4. Comparison of the multiple CUSUM charts and the FDR-adjusted CUSUM chart (Markov chain method). The mean shift magnitudes are equal. $N = 30, ARL_0 = 700, \alpha = 0.0168, h = 8.77$. Values in parentheses are for the multiple CUSUM charts

	Number of out-of-control stages								
	1			3			6		
δ	*ARL*	Power (%)	FDR (%)	ARL	Power (%)	FDR (%)	*ARL*	Power (%)	FDR (%)
0.5	293.0 (292.9)	57.1 (57.0)	0.15 (0.15)	66.1 (66.1)	31.2 (30.6)	0.13 (0.13)	34.7 (34.7)	17.2 (16.4)	0.09 (0.09)
1.0	45.9 (45.9)	93.5 (93.3)	0.15 (0.15)	15.3 (15.3)	36.7 (34.3)	0.09 (0.08)	11.0 (11.0)	22.1 (18.5)	0.04 (0.04)
1.5	19.4 (19.4)	97.7 (97.4)	0.15 (0.14)	8.7 (8.7)	41.1 (36.6)	0.07 (0.05)	6.7 (6.8)	27.4 (20.9)	0.03 (0.01)
2.0	12.1 (12.1)	98.6 (98.5)	0.15 (0.14)	6.1 (6.2)	44.4 (39.2)	0.03 (0.02)	5.0 (5.0)	33.9 (24.7)	0.02 (0.01)
3.0	7.0 (7.0)	99.7 (99.5)	0.12 (0.10)	4.0 (4.0)	51.8 (45.1)	0.03 (0.02)	3.3 (3.4)	46.0 (33.3)	0.02 (0.00)
4.0	4.9 (4.9)	99.9 (99.8)	0.11 (0.07)	3.0 (3.0)	58.4 (51.0)	0.04 (0.01)	2.6 (2.7)	61.5 (48.2)	0.03 (0.01)
5.0	3.9 (3.9)	100 (99.9)	0.09 (0.05)	2.4 (2.5)	62.0 (55.1)	0.08 (0.01)	2.0 (2.0)	64.4 (41.5)	0.02 (0.00)

Table 5. Comparison of the multiple CUSUM charts and the FDR-adjusted CUSUM chart (Brownian motion method). The mean shift magnitudes are equal. $N = 30$, $ARL_0 = 700$, $\alpha = 0.044$, $h = 8.77$. Values in parentheses are for the multiple CUSUM charts

	Number of out-of-control stages								
	1			3			6		
δ	*ARL*	Power (%)	FDR (%)	*ARL*	Power (%)	FDR (%)	*ARL*	Power (%)	FDR (%)
0.5	292.5 (293.3)	57.1 (57.1)	0.15 (0.15)	65.3 (65.4)	31.5 (30.7)	0.13 (0.13)	34.6 (34.7)	17.7 (16.4)	0.10 (0.09)
1.0	46.4 (46.4)	93.2 (92.9)	0.16 (0.16)	15.2 (15.2)	37.8 (34.3)	0.11 (0.10)	11.0 (11.1)	23.6 (18.6)	0.05 (0.04)
1.5	19.5 (19.5)	97.5 (97.1)	0.17 (0.16)	8.6 (8.7)	42.3 (36.6)	0.08 (0.06)	6.7 (6.8)	29.7 (21.0)	0.04 (0.03)
2.0	12.2 (12.2)	98.8 (98.5)	0.16 (0.13)	6.1 (6.2)	46.2 (39.1)	0.05 (0.03)	4.9 (5.0)	36.6 (24.5)	0.02 (0.01)
3.0	7.0 (7.0)	99.7 (99.6)	0.14 (0.10)	3.9 (4.0)	53.8 (44.9)	0.06 (0.02)	3.3 (3.4)	49.5 (32.8)	0.02 (0.00)
4.0	4.9 (4.9)	99.9 (99.8)	0.12 (0.07)	3.0 (3.0)	61.2 (51.1)	0.06 (0.01)	2.6 (2.7)	63.6 (48.7)	0.05 (0.00)
5.0	3.9 (3.9)	100 (99.9)	0.14 (0.07)	2.4 (2.4)	63.1 (54.6)	0.08 (0.01)	2.0 (2.0)	70.3 (41.7)	0.02 (0.00)

Table 6. Comparison of the multiple CUSUM charts and the FDR-adjusted CUSUM chart (Corrected Brownian motion method). The mean shift magnitudes are equal. $N = 30$, $ARL_0 = 700$, $\alpha = 0.025$, $h = 8.77$. Values in parentheses are for the multiple CUSUM charts

	Number of out-of-control stages								
	1			3			6		
δ	*ARL*	Power (%)	FDR (%)	*ARL*	Power (%)	FDR (%)	*ARL*	Power (%)	FDR (%)
0.5	292.7 (292.9)	57.3 (57.1)	0.15 (0.15)	66.3 (66.3)	31.4 (30.6)	0.13 (0.13)	34.6 (34.7)	17.6 (16.4)	0.09 (0.09)
1.0	46.1 (46.1)	92.6 (92.3)	0.18 (0.17)	15.2 (15.2)	37.9 (34.3)	0.11 (0.09)	10.9 (11.0)	23.8 (18.6)	0.06 (0.04)
1.5	19.5 (19.5)	97.3 (97.1)	0.17 (0.16)	8.7 (8.7)	42.5 (36.8)	0.07 (0.05)	6.7 (6.8)	29.9 (21.2)	0.03 (0.01)
2.0	12.1 (12.1)	98.7 (98.5)	0.16 (0.14)	6.1 (6.1)	46.4 (39.0)	0.07 (0.04)	4.9 (5.0)	36.8 (24.7)	0.03 (0.01)
3.0	6.9 (6.9)	99.6 (99.5)	0.14 (0.10)	3.9 (4.0)	53.6 (44.7)	0.05 (0.02)	3.3 (3.4)	49.7 (32.9)	0.03 (0.00)
4.0	4.9 (4.9)	99.9 (99.8)	0.12 (0.07)	3.0 (3.0)	61.1 (50.8)	0.06 (0.01)	2.6 (2.7)	62.9 (48.1)	0.06 (0.00)
5.0	3.9 (3.9)	99.9 (99.9)	0.12 (0.06)	2.4 (2.4)	63.6 (54.6)	0.09 (0.01)	2.0 (2.0)	70.2 (41.6)	0.02 (0.00)

Table 7. Comparison of the multiple CUSUM charts and the FDR-adjusted CUSUM chart (Markov chain method). The mean shift magnitudes vary. $N = 30$, $ARL_0 = 700$, $\alpha = 0.0168$, $h = 8.77$. Values in parentheses are for the multiple CUSUM charts

	Number of out-of-control stages					
	3			6		
δ	*ARL*	Power (%)	FDR (%)	*ARL*	Power (%)	FDR (%)
Category I	8.63 (8.67)	40.69 (36.62)	0.06 (0.05)	6.71 (6.76)	27.30 (21.02)	0.03 (0.02)
Category II	4.79 (4.81)	47.97 (41.41)	0.05 (0.02)	3.96 (4.01)	40.86 (28.75)	0.02 (0.00)
Category III	3.39 (3.41)	54.72 (47.62)	0.04 (0.01)	2.93 (2.96)	56.78 (38.73)	0.02 (0.00)

Table 8. Comparison of the multiple CUSUM charts and the FDR-adjusted CUSUM chart (Brownian motion method). The mean shift magnitudes vary. $N = 30$, $ARL_0 = 700$, $\alpha = 0.044$, $h = 8.77$. Values in parentheses are for the multiple CUSUM charts

	Number of out-of-control stages					
	3			6		
δ	*ARL*	Power (%)	FDR (%)	*ARL*	Power (%)	FDR (%)
Category I	8.64 (8.69)	42.15 (36.48)	0.06 (0.04)	6.66 (6.76)	29.69 (21.12)	0.04 (0.02)
Category II	4.77 (4.81)	49.96 (41.49)	0.05 (0.01)	3.93 (4.00)	44.10 (28.54)	0.03 (0.01)
Category III	3.39 (3.42)	57.26 (47.74)	0.06 (0.01)	2.92 (2.96)	61.65 (38.94)	0.04 (0.00)

Table 9. Comparison of the multiple CUSUM charts and the FDR-adjusted CUSUM chart (Corrected Brownian motion). The mean shift magnitudes vary. $N = 30$, $ARL_0 = 700$, $\alpha = 0.025$, $h = 8.77$. Values in parentheses are for the multiple CUSUM charts

	Number of out-of-control stages					
	3			6		
δ	*ARL*	Power (%)	FDR (%)	*ARL*	Power (%)	FDR (%)
Category I	8.63 (8.69)	42.14 (36.49)	0.08 (0.06)	6.67 (6.77)	30.02 (21.24)	0.03 (0.01)
Category II	4.77 (4.81)	50.25 (41.32)	0.07 (0.04)	3.93 (4.01)	44.42 (28.91)	0.03 (0.01)
Category III	3.38 (3.41)	56.73 (47.49)	0.06 (0.01)	2.92 (2.95)	61.14 (38.89)	0.02 (0.00)

chart is used of the Shewhart chart.

Table 6 gives the results for the FDR-adjusted CUSUM chart based on the corrected Brownian motion method. When only the first stage goes out of control, two types of CUSUM charts have similar performance, and their fault identification capability is quite satisfactory. For example, when the mean shift is 1.0, the average power of both methods is as high as 93%. When the number of faulty stages increases, the FDR-adjusted CUSUM chart outperforms the multiple CUSUM charts, and the superiority becomes even more obvious as the mean shift magnitude increases. For instance, when the first three stages experience a mean shift of magnitude four, the average power of the FDR-adjusted CUSUM chart is 61%, compared with only 50% for the multiple CUSUM charts. As the number of faulty stages increases to six while the mean shift increases to five, the average power of the FDR-adjusted CUSUM chart remains as high as 70%, whereas that of the multiple CUSUM charts is only around 42%.

Tables 7, 8, and 9 compare the performance of the multiple CUSUM charts and the FDR-adjusted CUSUM chart with varying mean shift magnitudes. The superiority of the FDR-adjusted CUSUM chart is still noticeable even in light of average power. This superiority becomes even more obvious as the number of faulty stages and the difference in the mean shifts increase; for example, for category II mean shifts, when the first three stages go out of control, the average power of the FDR-adjusted CUSUM chart is 50%, whereas that of the multiple Shewhart charts is only 41%, and when the first six stages go out of control and category III mean shifts occur, the average power of the FDR-adjusted CUSUM chart is 61%, compared with only 39% for the multiple CUSUM charts.

Allocation of faulty stages will affect the numerical results. Nevertheless, the FDR-adjusted CUSUM chart always has a clear advantage over the multiple CUSUM charts.

In summary, the FDR-adjusted CUSUM chart performs much better than the multiple CUSUM charts, especially when more than one stage goes out of control or the mean shifts of different size occur simultaneously.

6.5 The Effect of Process Parameters *A* and *C*

Similar to Section 5.2, here we report the effect of the process parameters (A_n, C_n) on the performance of the FDR-adjusted CUSUM chart and the multiple CUSUM charts. The value of A_n is assumed to be known and to vary from 0.8 to 1.0 and 1.2, as is the value of C_n. All other parameters are set the same as in Section 5.2.

Section 6.3 explains that the corrected Brownian motion method not only has smaller MSE, but also is computationally efficient. The comparison results given in Section 6.4 also show that the FDR-adjusted CUSUM chart is quite robust to three different approximation methods; thus we give only the results for the FDR-adjusted CUSUM chart based on the corrected Brownian motion method.

Figures 5 and 6 graphically compare the average power of the FDR-adjusted CUSUM chart and the multiple CUSUM charts. Figure 5 shows the scenario in which the first one, three or six stages in the process are faulty stages with equal shift magnitudes, and Figure 6 shows the case with varying mean shifts.

Similar to the results given in Section 5.2, Figures 5 and 6 show that if the values of (A_n, C_n) do not change significantly, then the performance of the FDR-adjusted CUSUM chart and

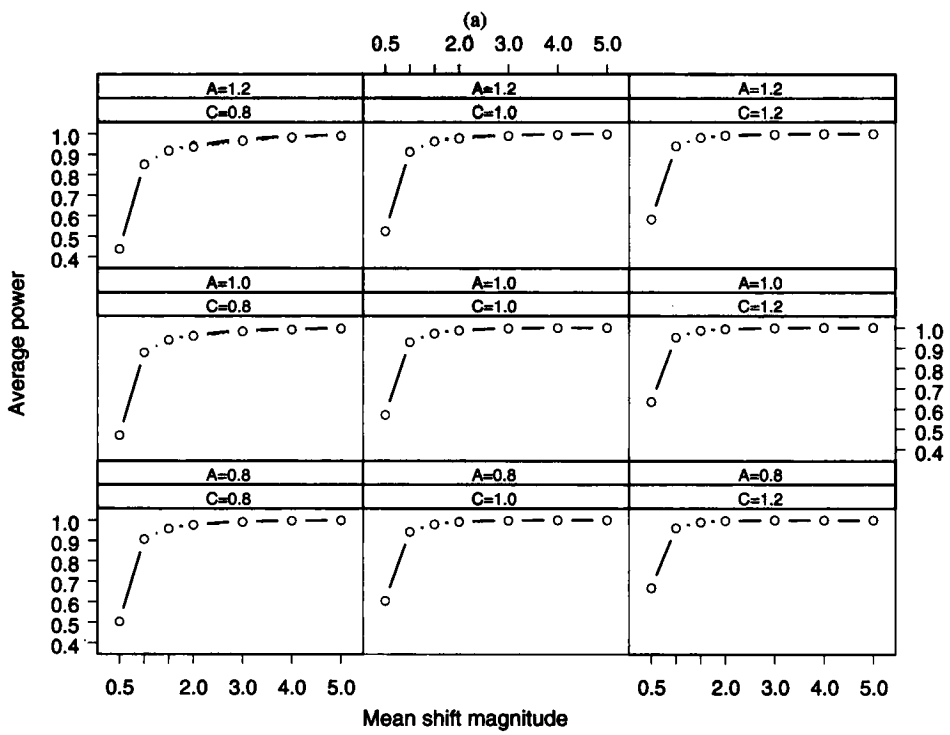

Figure 5. Average power of the FDR-adjusted CUSUM chart (solid lines with solid circles) and the multiple CUSUM charts (dashed lines with empty circles) with varying process parameters, A_n and C_n. The mean shifts of different stages are equal. (a) Number of faulty stages = 1. (b) Number of faulty stage = 3. (c) Number of faulty stage = 6.

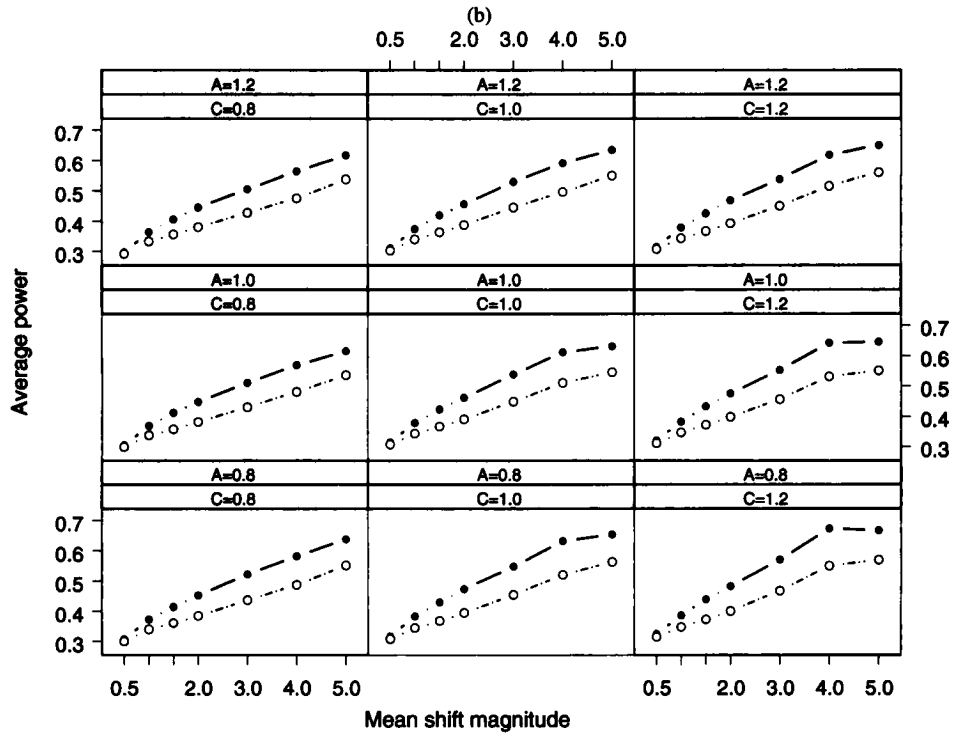

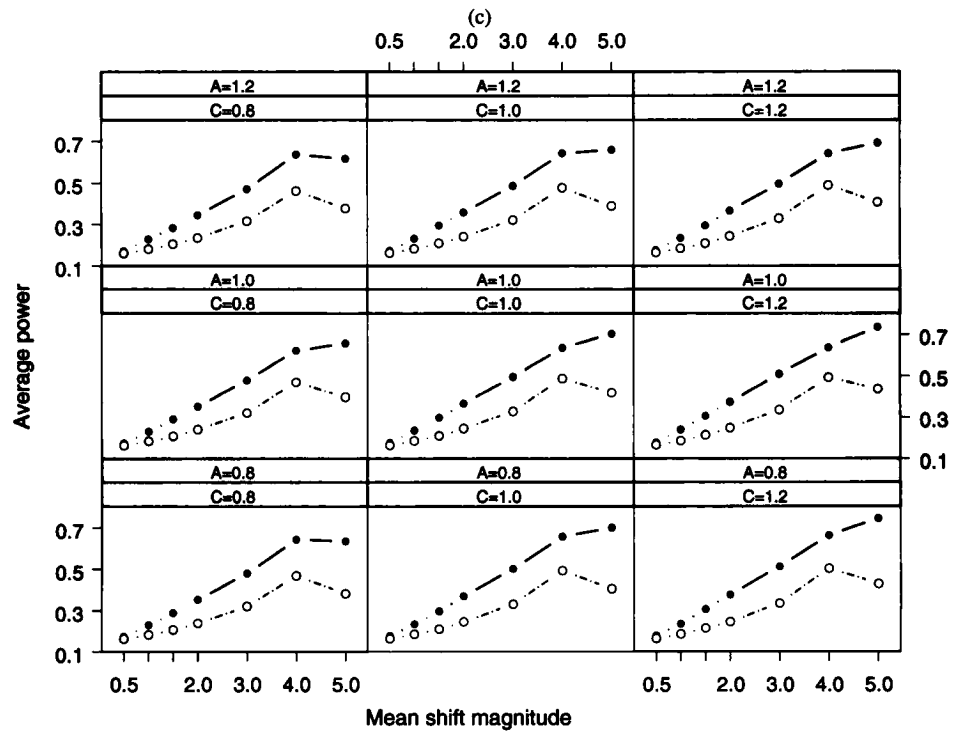

Figure 5. (Continued.)

the multiple CUSUM charts will not change significantly. In Figure 5, we assume that the faulty stages share the same mean shift magnitude. When only the first stage goes out of control, the two control schemes perform quite similarly, but when more than one stage goes out of control, regardless of the variation in the process parameters, the superiority of the FDR-adjusted CUSUM chart is quite obvious.

Figure 6 illustrates the varying mean shift scenario. We consider the first three or six stages to be faulty stages that experience category I, category II, or category III mean shifts. For category I mean shifts, when there are three faulty stages, the average power of the FDR-adjusted CUSUM chart exceeds that of the multiple CUSUM charts by an average of 6%, with six faulty stages, this figure rises to 10%. The superiority of the FDR-adjusted CUSUM chart is even more evident for category II mean shifts, with average power exceeding that of the multiple CUSUM charts by 10% for three faulty stages and by 15% for six faulty stages. When the difference between the mean

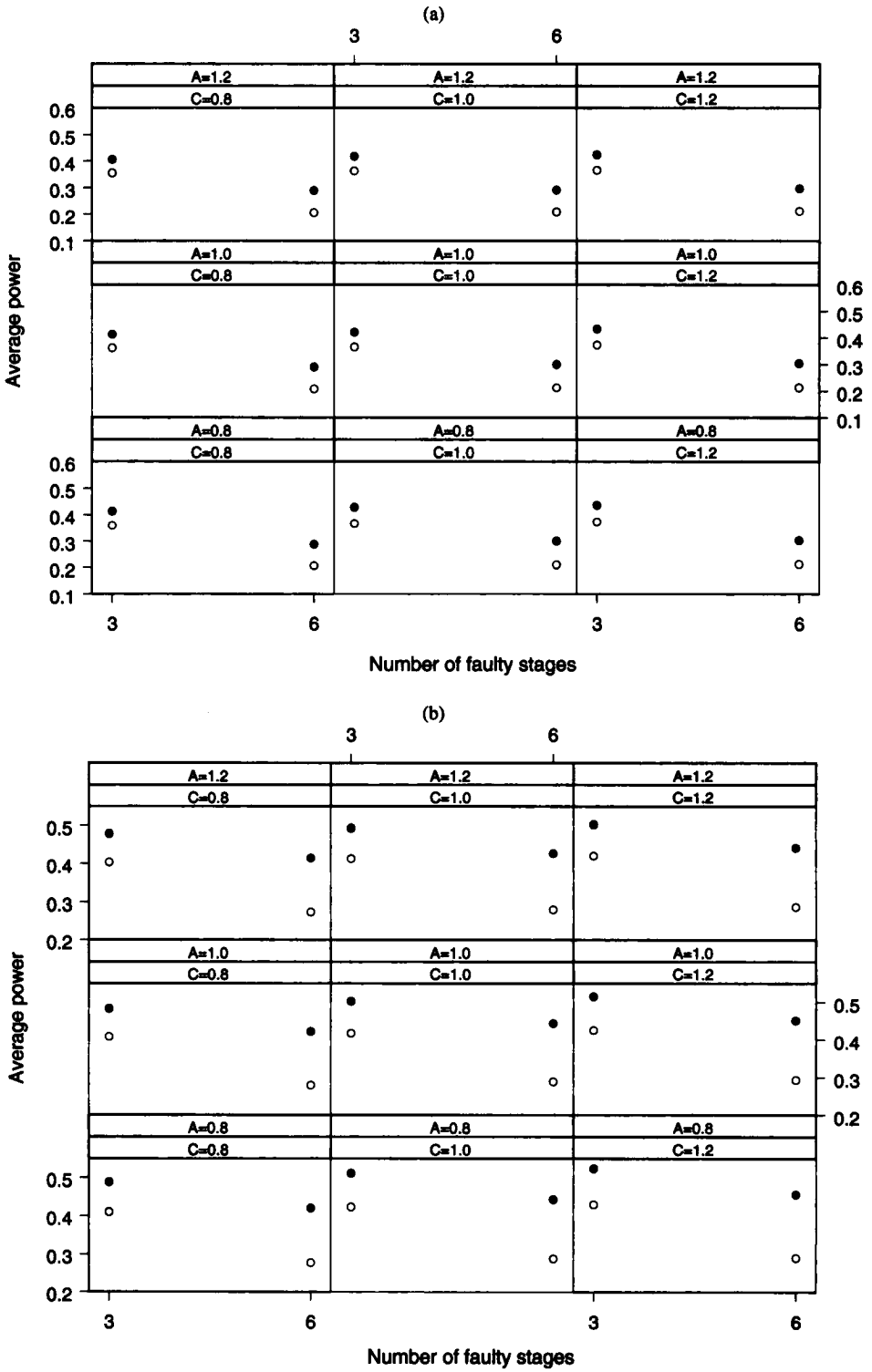

Figure 6. Average power of the FDR-adjusted CUSUM chart (solid dots) and the multiple CUSUM charts (circles) with varying process parameters, A_n and C_n and varying mean shifts. (a) Category I mean shifts. (b) Category II mean shifts. (c) Category III mean shifts.

shifts is as large as 1.5, as in category III mean shifts, this superiority increases to 10% and 20%, respectively.

7. MOTIVATING EXAMPLE REVISITED

Here we revisit the motivating example involving the transmission of variation in a multistage automobile hood manufacturing process (Lawless, MacKay, and Robinson 1999; Agrawal, Lawless, and MacKay 1999) and use this example to demonstrate the implementation of the FDR-adjusted control schemes. Note that the process involves four stages: hanging, painting, hardware, and finesse. More specifically, the flushness of 19 car hoods at four measurement locations (left front, right front, left rear, and right rear) is measured in each of the

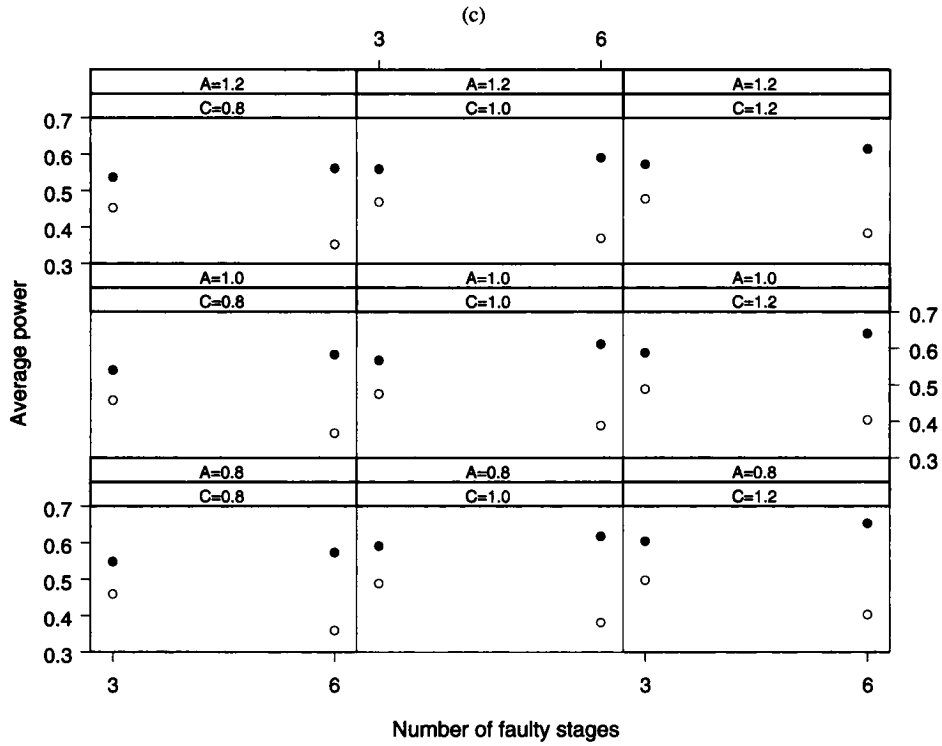

Figure 6. (Continued.)

four operational steps. For illustration, we focus on the measurements collected from one of the four locations, the right rear. The state-space model for this multistage process is given in (2):

$$y_i = x_i + v_i,$$
$$x_{i+1} = \beta_i x_i + \omega_i, \qquad i = 1, 2, 3, 4. \tag{23}$$

As we can see, model (23) has the same form as model (3) with $A_i = \beta_i$, $C_i = 1$.

We assume that $\sigma_v = 0.1$. Based on model (23), we simulate new observations, y_i's, for another $m = 19$ cars with the same initial states described by Lawless, Mackay, and Robinson (1999). The first 10 cars are observed under normal conditions, as described by model (23). We add a mean shift of $\delta = 3$ to the second and third stages for the next nine cars. Use of the FDR-adjusted CUSUM chart and the multiple CUSUM charts are used to monitor the car hood manufacturing process and identify the faulty stages is implemented as follows:

1. Given $ARL_0 = 700$ and $N = 4$, the FDR-adjusted CUSUM chart and the multiple CUSUM charts with reference values $k = \delta/2 = 1.5$ are constructed. Their control limits, $\alpha = 0.051$ and $h = 6.77$, are obtained by simulation.
2. For product j, calculate the standardized one-step-ahead forecast errors of the 19 cars based on model (23) by (5), $\{e_{1,j}, e_{2,j}, e_{3,j}, e_{4,j}, j = 1, 2, \ldots, 19\}$.
3. Calculate $S^+_{1,j}, S^-_{1,j}, S^+_{2,j}, S^-_{2,j}, S^+_{3,j}, S^-_{3,j}, S^+_{4,j}, S^-_{4,j}$ based on (12).
4. For the multiple CUSUM charts, keep on sampling until any $S^+_{n,j}$ or $S^-_{n,j}$ falls beyond h. The stages associated with such $S^+_{n,j}$ or $S^-_{n,j}$ are diagnosed as faulty stages.
5. For the FDR-adjusted CUSUM chart,
   a) Calculate $\{p^+_{n,j}$ and $p^-_{n,j}, n = 1, 2, 3, 4\}$ by (21) for each stage; these are the p-values of $S^+_{n,j}$ and $S^-_{n,j}$.
   b) Order the p-values $\{p^+_{n,j}$ and $p^-_{n,j}, n = 1, 2, 3, 4\}$ as $p_{(1)}, p_{(2)}, \ldots, p_{(8)}$ in ascending order.
   c) Calculate $l = \max\{n : p_{(n)} \le \frac{n\alpha}{8\sum_{i=1}^{8} 1/i}, 1 \le n \le 8\}$. If $l > 0$, the process is determined to be out of control, and all of the stages associated with $\{p_{(n)}, n = 1, 2, \ldots, l\}$ are diagnosed as faulty stages. Otherwise, continue to sample.

After 1 million Monte Carlo simulation runs, the average power of the FDR-adjusted CUSUM chart is approximately 67%, 5% higher than that of the multiple CUSUM charts. This example further demonstrates that the FDR-adjusted CUSUM chart is better at identifying faulty stages in a multistage process.

8. CONCLUSION

In this work, we have formulated multistage process monitoring and fault identification into a multiple hypotheses testing problem. Based on a novel multiple hypotheses testing method, the FDR control procedure and two multistage process control and diagnosis schemes, the FDR-adjusted Shewhart chart and CUSUM chart, were established. To apply FDR control procedures, the distributions of the Shewhart and CUSUM control statistics were investigated. In particular, three methods for approximating the distribution of the CUSUM statistic based on Markov chain and Brownian motion theories were proposed. Through Monte Carlo simulations, the newly proposed methods exhibited higher average power than the multiple Shewhart and CUSUM charts. We also investigated the effect of process

parameters in the state-space model on the new control and diagnosis schemes.

The introduction of FDR control in multistage process monitoring and diagnosis opens up a potentially fruitful field for future research. First, an exponentially weighted moving average chart (EWMA; Roberts 1959) based on FDR control could be devised similarly. Likewise, whenever more than one quality characteristic needs to be monitored in each stage, FDR-adjusted multiple EWMA charts (Lowry et al. 1992) and multiple CUSUM charts (Woodall and Ncube 1985) charts could be established. Second, the properties of propagated shifts require further analysis, and their influence on the power of the proposed methods remains to be investigated. In addition, the uncertainty of the parameters may affect the performance of the FDR-adjusted control schemes. Last but not least, for multistage processes that may be described by regression models other than state-space models, the regression-adjusted chart and cause-selecting chart complemented with FDR control are more statistically appealing.

FDR control could be further extended beyond multistage process monitoring and fault identification to multivariate quality control and signal interpretation. Whenever more than one chart is used simultaneously (e.g., in controlling the mean and/or variance of several variables), controlling the FDR, rather than the type I error rate of the multiple charts, guarantees higher detection power as well.

ACKNOWLEDGMENTS

This research was supported by RGC Competitive Earmarked Research Grants 620606 and 620707. The authors thank the editor, associate editor, and two anonymous referees for their many helpful comments that have resulted in significant improvements in the article. They also thank to Bill Woodall for his constructive comments and suggestions on an earlier version of the manuscript. This work was initiated when Tsung was a visiting scholar at Stanford University; their hospitality is appreciated. Tsung is especially thankful to Trevor Hastie, Tze Leung Lai, Robert Tibshirani, Wing Hung Wong, and Peter Glynn at Stanford for their help and advice.

APPENDIX A: LIMITING DISTRIBUTION OF CUSUM STATISTICS

In this article the limiting distribution of the one-sided CUSUM statistic, $S_j^+ = \max\{0, S_{j-1}^+ + x_j - k\}$ with $S_0^+ = 0$, is calculated by the Markov chain method. Here x_j is assumed to be a random observation from a normal distribution, X. The distribution of X is assumed to be standard normal when the process is in control. We represent the scheme by a Markov chain having $r+1$ states labeled $E_0, E_1, \ldots, E_r$. For the upper-sided CUSUM chart based on S_j^+, the intervals are $(-\infty, \varpi/2), [\varpi/2, 3\varpi/2), \ldots, [(n-1/2)\varpi, (n+1/2)\varpi), \ldots, [(r-1/2)\varpi, +\infty)$, where $r+1$ is the number of the states and $\varpi = c/r$, where c is a very large positive real number that guarantees that the probability, $\Pr(S_j^+ \geq c)$, is trivial. The values in each interval that are used to represent the states that are chosen to be $0, \varpi, 2\varpi, \ldots,$ and $r\varpi$. The transition matrix, $\mathbf{P} = (p_{ij})_{(r+1)\times(r+1)}$, is determined only by the underlying process distribution of X. The transition probability is defined as follows:

$$\begin{aligned} p_{i0} &= \Pr(E_i \to E_0) = \Pr(X - k + i\varpi \in (-\infty, \varpi/2)) \\ &= \Pr(X \in (-\infty, -i\varpi + \varpi/2 + k)), \\ p_{ij} &= \Pr(E_i \to E_j) \\ &= \Pr\big(X - k + i\varpi \in (j\varpi - \varpi/2, j\varpi + \varpi/2)\big) \\ &= \Pr\big(X \in ((j-i)\varpi - \varpi/2 + k), ((j-i)\varpi + \varpi/2 + k)\big), \\ p_{ir} &= \Pr(E_i \to E_r) = \Pr(X - k + i\varpi \in (r\varpi - \varpi/2, +\infty)) \\ &= \Pr\big(X \in ((r-i)\varpi - \varpi/2 + k, +\infty)\big). \end{aligned}$$

Let $\{\pi_i, i = 0, 1, \ldots, r\}$ denote the limiting probability of the Markov chain. π_i can be viewed as the probability that the Markov chain falls at state i. Because S_j^+ forms an irreducible aperiodic and positive recurrent Markov chain, S_j^+ has a unique stationary distribution. Grounded in Markov chain theory, $\{\pi_i, i = 0, 1, \ldots, r\}$ can be computed as

$$\pi = \pi \mathbf{P}, \qquad \sum_{i=0}^{r} \pi_i = 1, \tag{24}$$

where $\pi = (\pi_0, \pi_1, \ldots, \pi_r)$. There are $r+2$ equations in total. Based on the properties of transition matrix $\mathbf{P}$, one of the equations among the first $r+1$ equations is redundant. We can arbitrarily delete one equation from the first $r+1$ equations, then easily solve equation (24).

We use a Fortran program to get $\{\pi_i, i = 0, 1, \ldots, r\}$. We use $c = 15$ and divide the region $(0, +\infty)$ into $r+1 = 3{,}001$ subintervals. Based on π_i, the p-value of the CUSUM statistic can be calculated. For $x > 0$,

$$\begin{aligned} \Pr(S_j^+ \geq x) &= \sum_{i=a}^{r} \pi_i, \\ a &= \{l : x \in E_l,\ l = 0, 1, \ldots, r\}. \end{aligned} \tag{25}$$

APPENDIX B: APPROXIMATED p-VALUES OF CUSUM STATISTICS BASES ON BROWNIAN MOTION THEORY

Suppose that X follows a standard normal distribution with mean 0 and variance 1, $x_1, x_2, \ldots$ are independent random observations drawn from X. also suppose that $k > 0$ and $S_j = \sum_{i=1}^{j}(x_i - k)$. Then $E(X - k) = -k = \mu_0 < 0$.

Because $X - k$ follows $\mathrm{N}(\mu_0, 1)$, the density function of $X - k$ can be written as

$$\frac{1}{2} e^{-x^2/2 + \mu_0 x - \psi(\mu_0)}, \tag{26}$$

where $\psi(\mu) = \mu^2/2$.

Siegmund (1985) proved that if there exists $\mu_1 > 0$ such that $\psi(\mu_0) = \psi(\mu_1)$, then, given $-B \leq 0 < A$, the probability that S_j hits A before hitting $-B$ can be computed as

$$\Pr_{\mu_0}(S_j \text{ hits } A \text{ before } -B) \cong \frac{e^{-\Delta(A+\rho)} - e^{-\Delta(A+B+2\rho)}}{1 - e^{-\Delta(A+B+2\rho)}}, \tag{27}$$

where $\Delta = \mu_1 - \mu_0$, $\rho = 0.583$.

Obviously, we can slightly modify expression (27) and obtain a useful result for our research. To make $\psi(\mu_0) = \psi(\mu_1)$ hold, μ_1 must be k. Then $\Delta = \mu_1 - \mu_0 = 2k$. Expression (27) can be written as

$$\Pr_{\mu_0}(S_j \text{ hits } A \text{ before } -B) \cong \frac{e^{-2k(A+\rho)} - e^{-2k(A+B+2\rho)}}{1 - e^{-2k(A+B+2\rho)}}. \tag{28}$$

Let B approach infinity. The probability that S_j hits A can be easily calculated as

$$\Pr_{\mu_0}(S_j \geq A) \cong e^{-2k(A+\rho)}. \tag{29}$$

[Received July 2006. Revised August 2008.]

REFERENCES

Agrawal, R., Lawless, J. F., and Mackay, R. J. (1999), "Analysis of Variation Transmission in Manufacturing Processes—Part II," *Journal of Quality Technology*, 31, 143–154.

Bagshaw, M., and Johnson, R. A. (1975), "The Influence of Reference Values and Estimated Variance on the ARL of CUSUM Tests," *Journal of the Royal Statistical Society*, Ser. B, 37, 413–420.

Basseville, M., and Nikiforov, I. V. (1993), *Detection of Abrupt Changes: Theory and Application*, Englewood Cliffs, NJ: Prentice Hall.

Benjamini, Y., and Hochberg, Y. (1995), "Controlling the False Discovery Rate—A Practical and Powerful Approach to Multiple Testing," *Journal of the Royal Statistical Society*, Ser. B, 57, 289–300.

——— (2000), "On the Adaptive Control of the False Discovery Rate in Multiple Testing With Independent Statistics," *Journal of Educational and Behavioral Statistics*, 25, 60–83.

Benjamini, Y., and Kling, Y. (1999), "A Look at Statistical Process Control Through the p-Values," Technical Report RP–SOR-99-08, Tel Aviv University, Israel.

Benjamini, Y., and Liu, W. (1999), "A Step-Down Multiple Hypotheses Procedure That Controls the False Discovery Rate Under Independence," *Journal of Statistical Planning and Inference*, 82, 163–170.

Benjamini, Y., and Yekutieli, D. (2001), "The Control of the False Discovery Rate in Multiple Testing Under Dependency," *Annals of Statistics*, 29, 1165–1188.

——— (2005), "False Discovery Rate-Adjusted Multiple Confidence Intervals for Selected Parameters," *Journal of the American Statistical Association*, 469, 71–81.

Benjamini, Y., Krieger, A. M., and Yekutieli, D. (2006), "Adaptive Linear Step-Up Procedures That Control the False Discovery Rate," *Biometrika*, 93, 491–507.

Brook, D., and Evans, D. A. (1972), "An Approach to the Probability Distribution of CUSUM Run Length," *Biometrika*, 59, 539–549.

Ding, Y., Ceglarek, D., and Shi, J. (2002), "Fault Diagnosis of Multistage Manufacturing Processes by Using State Space Approach," *Journal of Manufacturing Science and Engineering—Transactions of the ASME*, 124, 313–322.

Ding, Y., Jin, J., Ceglarek, D., and Shi, J. (2005), "Process-Oriented Tolerancing for Multi-Station Assembly Systems," *IIE Transactions*, 37, 493–508.

Ding, Y., Shi, J., and Ceglarek, D. (2002), "Diagnosability Analysis of Multi-station Manufacturing Processes," *ASME Transactions, Journal of Dynamic Systems, Measurement and Control*, 124, 1–33.

Djurdjanovic, D., and Ni, J. (2001), "Linear State Space Modeling of Dimensional Machining Errors," *Transactions of NAMRI/SME*, XXIX, 541–548.

Durbin, J., and Koopman, S. J. (2001), *Time Series Analysis by State Space Methods*, New York: Oxford University Press.

Fenner, J. S., Jeong, M. K., and Lu, J. C. (2005), "Optimal Automatic Control of Multistage Production Processes," *IEEE Transactions on Semiconductor Manufacturing*, 18, 94–103.

Genovese, C., and Wasserman, L. (2002), "Operating Characteristics and Extensions of the False Discovery Rate Procedure," *Journal of the Royal Statistical Society*, Ser. B, 64, 499–517.

Grant, G. R., Liu, J. M., and Stoeckert, C. J. (2005), "A Practical False Discovery Rate Approach to Identifying Patterns of Differential Expression in Microarray Data," *Bioinformatics*, 21, 2684–2690.

Grigg, O. A., and Spiegelhalter, D. J. (2005), "Random-Effects CUSUMs to Monitor Hospital Mortality," in *Statistical Solutions to Modern Problems: Proceedings of the 20th International Workshop on Statistical Modeling*, Sydney: University of Western Sydney Press, pp. 239–246.

Hauck, D. J., Runger, G. C., and Montgomery, D. C. (1999), "Multivariate Statistical Processes Monitoring and Diagnosis With Grouped Regression—Adjusted Variables," *Communications in Statistics—Simulation and Computation*, 28, 309–328.

Hawkins, D. M. (1991), "Multivariate Quality Control Based on Regression-Adjusted Variables," *Technometrics*, 33, 61–75.

——— (1993), "Regression Adjustment for Variables in Multivariate Quality Control," *Journal of Quality Technology*, 25, 170–182.

Huang, Q., and Shi, J. (2004), "Stream of Variation Modeling and Analysis of Serial-Parallel Multistage Manufacturing Systems," *Journal of Manufacturing Science and Engineering—Transactions of the ASME*, 126, 611–618.

Huang, Q., Zhou, S., and Shi, J. (2002), "Diagnosibility of Multi-Operational Machining Processes Through Variation Propagation Analysis," *Robotics and CIM Hournal*, 18, 233–239.

Jin, J., and Shi, J. (1999), "State Space Modeling of Sheet Metal Assembly for Dimensional Control," *Journal of Manufacturing Science and Engineering—Transactions of the ASME*, 121, 756–762.

Kim, T. S., and May, G. S. (1999), "Sequential Modeling of via Formation in Photosensitive Dielectric Materials for MCM–D Applications," *IEEE Transactions on Semiconductor Manufacturing*, 12, 345–352.

Lai, T. L. (2000), "Sequential Multiple Hypotheses Testing and Efficient Fault Detection-Isolation in Stochastic Systems," *IEEE Transactions on Information Theory*, 46, 595–608.

Lawless, J. F., Mackay, R. J., and Robinson, J. A. (1999), "Analysis of Variation Transmission in Manufacturing Processes—Part I," *Journal of Quality Technology*, 31, 131–142.

Lowry, C. A., Woodall, W. H., Champ, C. W., and Rigdon, S. E. (1992), "A Multivariate Exponentially Weighted Moving Average Control Chart," *Technometrics*, 34, 46–53.

Marshall, C., Best, N., Bottle, A., and Ayln, P. (2004), "Statistical Issues in the Prospective Monitoring of Health Outcomes Across Multiple Units," *Journal of the Royal Statistical Society*, Ser. A, 167, 541–559.

Page, E. S. (1954), "Continuous Inspection Schemes," *Biometrika*, 41, 100–115.

Qian, H. R., and Huang, S. G. (2005), "Comparison of False Discovery Rate Methods in Identifying Genes With Differential Expression," *Genomics*, 86, 495–503.

Rao, S., Strojwas, A. J., Lehoczky, J. P., and Schervish, M. J. (1996), "Monitoring Multistage Integrated Circuit Fabrication Processes," *IEEE Transactions on Semiconductor Manufacturing*, 9, 495–505.

Reiner, A., Yekutieli, D., and Benjamini, Y. (2003), "Identifying Differentially Expressed Genes Using False Discovery Rate Controlling Procedures," *Bioinformatics*, 19, 368–375.

Roberts, S. W. (1959), "Control Charts Based on Geometric Moving Averages," *Technometrics*, 1, 239–250.

Ross, S. M. (1996), *Stochastic Process* (2nd ed.), New York: Wiley.

Shewhart, W. A. (1931), *Economic Control of Quality of Manufactured Product*, New York: Van Nostrand.

Shi, J. (2007), *Stream of Variation Modeling and Analysis for Multistage Manufacturing Processes*, Boca Raton, FL: CRC Press/Taylor & Francis.

Shu, L. J., and Tsung, F. (2003), "On Multistage Statistical Process Control," *Journal of Chinese Institute of Industrial Engineers*, 20, 1–8.

Shu, L. J., Apley, D. W., and Tsung, F. (2003), "Autocorrelated Process Monitoring Using Triggered Cuscore Charts," *Quality and Reliability Engineering International*, 18, 411–421.

Shu, L. J., Tsung, F., and Kapur, K. C. (2004), "Design of Multiple Cause-Selecting Charts for Multistage Processes With Model Uncertainty," *Quality Engineering*, 16, 437–450.

Siegmund, D. (1985), *Sequential Analysis: Tests and Confidence Intervals*, New York: Springer.

Storey, J. D. (2001), "The Positive False Discovery Rate: A Bayesian Interpretation and the q-Value," *Annals of Statistics*, 31, 2013–2035.

——— (2002), "A Direct Approach to False Discovery Rates," *Journal of the Royal Statistical Society*, Ser. B, 64, 479–498.

Storey, J. D., Taylor, J. E., and Siegmund, D. (2004), "Strong Control, Conservative Point Estimation and Simultaneous Conservative Consistency of False Discovery Rates: A Unified Approach," *Journal of the Royal Statistical Society*, Ser. B, 66, 187–205.

Tripolski Kimel, M., Benjamini, Y., and Steinberg, D. M. (2008), "The False Discovery Rate for Multiple Testing in Factorial Experiments," *Technometrics*, 50, 32–39.

Tusher, V. G., Tibshirani, R., and Chu, G. (2001), "Significance Analysis of Microarrays Applied to the Ionizing Radiation Response," *Proceedings of the National Academy of Sciences of the United States of America*, 98, 5116–5121.

Wade, M. R., and Woodall, W. H. (1993), "A Review and Analysis of Cause-Selecting Control Charts," *Journal of Quality Technology*, 25, 161–169.

Woodall, W. H. (2006), "The Use of Control Charts in Health-Care and Public-Health Surveillance," *Journal of Quality Technology*, 38, 89–104.

Woodall, W. H., and Ncube, M. M. (1985), "Multivariate CUSUM Quality-Control Procedures," *Technometrics*, 27, 285–292.

Xiang, L., and Tsung, F. (2008), "Statistical Monitoring of Multistage Processes Based on Engineering Models," *IIE Transactions*, 40, 957–970.

Zantek, P. F., Wright, G. P., and Plante, R. D. (2002), "Process and Product Improvement in Manufacturing Systems With Correlated Stages," *Management Science*, 48, 591–606.

——— (2006), "A Self-Starting Procedure for Monitoring Process Quality in Multistage Manufacturing Systems," *IIE Transactions*, 38, 293–308.

Zhang, G. X. (1984), "A New Type of Control Charts and a Theory of Diagnosis With Control Charts," in *Proceedings of World Quality Congress Transactions*, Milwaukee, WI: American Society for Quality Control, pp. 75–85.

——— (1985), "Cause-Selecting Control Charts—A New Type of Quality Control Charts," *The QR Journal*, 12, 221–225.

——— (1990), "A New Diagnosis Theory With Two Kinds of Quality," *Total Quality Management & Business Exellence*, 1, 249–258.

——— (1992), "Cause-Selecting Control Chart and Diagnosis, Theory and Practice," Aarhus School of Business, Dept. of Total Quality Management, Aarhus, Denmark.

Zhou, S., Ding, Y., Chen, Y., and Shi, J. (2003), "Diagnosability Study of Multistage Manufacturing Processes Based on Linear Mixed-Effects Models," *Technometrics*, 45, 312–325.

Zhou, S., Huang, Q., and Shi, J. (2003), "State Space Modeling of Dimensional Variation Propagation in Multistage Machining Process Using Differential Motion Vector," *IEEE Transactions on Robotics and Automation*, 19, 296–309.

Zou, C., and Tsung, F. (2008), "Directional MEWMA Schemes for Multistage Process Monitoring and Diagnosis," *Journal of Quality Technology*, 40, 407–427.

Zou, C., Tsung, F., and Liu, Y. (2008), "A Change Point Approach for Phase I Analysis in Multistage Processes," *Technometrics*, 50, 344–356.